



pubs.acs.org/IECR Review

Dual-Function Materials for CO₂ Capture and Conversion: A Review

Ibeh S. Omodolor,[†] Hope O. Otor,[†] Joseph A. Andonegui, Bryan J. Allen, and Ana C. Alba-Rubio*



Cite This: Ind. Eng. Chem. Res. 2020, 59, 17612-17631



ACCESS

Metrics & More

Article Recommendations

ABSTRACT: Anthropogenic emissions of CO_2 from industrial processes are considered the major cause of global warming and ocean acidification. To this end, different abatement strategies have been sought to capture CO_2 directly from various effluent sources. Carbon capture and sequestration (CCS) has been touted to solve this problem; however, due to the challenges associated with this approach, research efforts have been focused on the development of dual-function materials (DFMs) that can effectively capture and convert CO_2 to value-added products. In this review, we first describe existent CO_2 capture processes, followed by relevant CO_2 adsorbents. Then, we focus on the development of DFMs for CO_2 capture and conversion through various reaction pathways, such as methanation, reverse water-gas shift, and dry reforming. We also



elaborate on the challenges associated with these systems with emphasis on the stability and regenerability of the materials. Finally, some future perspectives and possible areas of study are highlighted.

1. INTRODUCTION

Increasing CO_2 emissions and atmospheric concentration has been considered the main cause of global warming.¹ In the US, for instance, the CO_2 emissions from energy-related systems have been projected to increase by 3% from 2013 to 2040, while the consumption is only expected to increase by 0.3% within the same time frame.² To this end, considerable research efforts have focused on the chemical transformation of CO_2 and its utilization as a carbon source for the production of fuels and commodity chemicals.³⁻⁷

Carbon capture and sequestration (CCS) has been widely reported as a means to mitigate the emissions of CO2 to the atmosphere, employing systems based on amine solvents, ionic liquids, solid sorbents, advanced membrane, and porous materials.^{8,9} CCS enables CO₂ to be concentrated, liquefied, and stored to minimize the emissions from large-scale industrial processes. If applied efficiently, this strategy has the potential to reduce CO₂ emissions from a conventional power plant by 80-90%.8 CCS systems are generally categorized as precombustion, oxy-fuel combustion, and postcombustion, based on the location of the capture system. 9,10 However, these are thermal swing sorption processes that rely on temperature variations for carbon capture and subsequent regeneration of the sorbent. In addition, these processes involve the transportation of compressed CO2 gas and subsequent storage in geological formations. Thus, making the processes highly energy intensive and less economically viable.

Owing to the challenges associated with these strategies for environmental CO₂ abatement, dual-function materials (DFMs) are currently being sought out as a means to capture and convert CO₂ to value-added products. DFMs contain both an adsorbent and a catalytic component for CO₂ capture and conversion, respectively. The adsorbent component, which usually consists of alkali metal oxides or carbonates, provides basic sites to capture CO2 directly from flue gas in exhaust systems; then, this can be converted on the same material to different value-added products, such as light hydrocarbons or commodity chemicals. DFMs also have the ability to efficiently concentrate CO₂ from very dilute streams such as the typical exhaust and waste gases from industrial plants. The use of DFMs can also ultimately eliminate the problems of CO₂ transportation and storage associated with CCS.

In this review, we first examine several oxides and carbonate-based adsorbents with excellent sorption capacities that have been combined with catalysts for the development of DFMs. Then, we critically discuss the different types of DFMs that have been used for the capture and valorization of CO_2 , with major emphasis on Ni, Ru, and Rh-based DFM

Received: May 6, 2020
Revised: August 14, 2020
Accepted: August 27, 2020
Published: August 27, 2020





systems. The use of these DFMs under simulated flue gas conditions is also elaborated in relation to different catalytic reactions. Further, focus is given to the effect of the different parameters on the capture capacity and catalytic activity of these materials. Lastly, some future directions and areas for study are highlighted.

2. CO₂ CAPTURE PROCESSES

Several thorough reviews on existing CO_2 capture processes can be found in the literature. For instance, Mondal et al. described recent technologies for CO_2 capture and separation from thermal power plant flue gas, ¹¹ and Al-Mamoori et al. ¹² reviewed the most recent advances on combined CO_2 capture and utilization, along with their associated challenges. This section summarizes the main technologies for capturing CO_2 and Table 1 compares them in terms of energy requirement, cost, CO_2 recovery, challenges, and areas of improvement.

Precombustion capture is a technique in which the fuel is reacted with air or oxygen, and sometimes with steam, to produce syngas (CO + H_2) as the major product, after which the CO produced is reacted with steam in a catalytic reactor to produce CO₂ and more H₂. Produced CO₂ is then separated either by physical or chemical absorption processes to produce hydrogen-rich fuel that can be used in boilers, furnaces, and gas turbines. On the other hand, oxy-fuel combustion involves the combustion of fuel in an atmosphere of oxygen with recycled CO2 and/or steam leading to a stream rich in CO₂ and water, which is easily separated by condensation. Oxy-fuel combustion can take place either by O₂ combustion with CO₂ recycle or by a chemical looping combustion (CLC) in which a solid material is used as the oxygen carrier. Another technique that can be employed in both precombustion or postcombustion is called calcium looping cycle. This process involves capturing CO₂ from flue gas by relying on the reversible reaction between CaO and CO₂ to form calcium carbonate.

Postcombustion strategies for CO₂ capture include absorption, membrane separation, and adsorption. Absorption involves the capture of CO2 from flue gas by reaction with a chemical solvent, typically amine-based solvents, such as aqueous solutions of mono-, di-, triamine, and di-isopropanol amine, among others. 11 Though the amine scrubbing system has been well developed for CO2 capture from flue gas, it suffers from some drawbacks, such as high energy cost for the regeneration of the absorbent due to the presence of water in the amine solution, low CO2 capture capacity, thermal degradation of the amines and losses through evaporation.¹⁴ To address the challenges associated with the use of amine solutions, amine-based solid sorbents have also been developed.¹⁵ Amine-functionalized solids require less energy when compared with amine solutions since no heat is required to evaporate water. Additionally, solid sorbents have lower heat capacities than aqueous amine solutions. Zhang et al. carried out a parametric study on the regeneration heat requirement of an amine-based solid material.¹⁶ While the calculated heat requirement for polyethyleneimine (PEI)/ silica was 2.46 GJ/tCO₂, the heat requirement was 3.9 GJ/ tCO₂ for a typical aqueous monoethanolamine (MEA) system, and 3.3 GJ/tCO₂ for an advanced MEA system with optimized process configuration. In addition, aminefunctionalized solids generally exhibit higher CO₂ capacity and higher resistance to flue gas contaminants. However, these solids have not been used at industrial scale because

Table 1. Comparison of Main Existing CO₂ Capture Technologies

				1 1 1 1 1 1 1 1 1 1 1 1 1 1 1 1 1 1 1 1	
				postcombustion	
	precombustion	oxy-fuel combustion	absorption	adsorption	membrane
nergy requirement	low regeneration energy (<50% of postcombustion)	low energy is required	$4-6 \text{ MJ/kgCO}_2$	2–3 MJ/kgCO ₂	0.5–6 MJ/kgCO ₂
	less expensive (requires smaller equipment size and capital cost)	moderately expensive	expensive	expensive	expensive
O ₂ recovery	92–93%	90-94%	%86-06	80-95%	%06-08
hallenges	requires an air separation unit	requires an air separation unit	corrosion	adsorbent attrition	high membrane cost
	unplanned shutdown due to process complexity	increased cost of recycling	huge energy requirement	high pressure drop	not suitable for high- temperature application
	high pressure operation	high temperature process	solvent degradation	greatly affected by trace impurities $(NO_{\omega} SO_{x})$	low CO ₂ selectivity
	temperature associated with heat transfer problems	requires more oxygen compared to precombustion	large volume of gas required	large volume of gas required	large volume of gas required
pportunities	improvement of the gasification stage	development of high-temperature resistant materials	development of corrosion inhibitors	use of hybrid processes (membrane-pressure swing adsorption)	use of composite membranes
	gas separation and new strategies for syngas cleaning		use of ionic liquids	development of newer adsorbents	use of hybrid membrane- cryogenic processes

CC

this technology is yet to be fully developed. Membrane separation technology is another postcombustion technique for capturing CO_2 ; however, further research is still needed to improve the stability, permeate purity, and recovery rate of the membranes. Adsorption is also a promising technique for capturing CO_2 due to its reduced energy requirement, ease of handling, and lack of corrosion problems. As a result, adsorbents have been combined with catalysts for the development of DFMs.

3. ADSORBENTS FOR CO2 CAPTURE

Adsorbents for the selective capture of CO2 from gas effluents need to meet several specifications, such as high adsorption capacity, low cost, low regeneration requirements, long-term stability, and fast kinetics. 18 Different materials, such as zeolites and activated carbons, have been stated to have a good affinity for CO2; but their sorption capacities are affected at high temperatures. 19 Others, such as mesoporous materials (SBA-15 and MCM-41) and metal organic frameworks (MOFs), have been reported to have good adsorption capabilities and cyclic stabilities when used at low temperatures, although they have also shown poor sorption capacities at high temperatures. ¹⁹ This is also the case of hydrotalcites, which have been reported as excellent adsorbents for CO₂, but possess low sorption capabilities for large scale industrial applications. ^{18,19} Some of the most promising adsorbents for DFMs are those based on calcium due to their excellent sorption capabilities at high temperatures. 18,20

In this review, we focus on oxides and carbonate-based adsorbents with good sorption capabilities that have been effectively combined with catalysts for the development of DFMs.

3.1. Oxide-Based Adsorbents. Calcium oxide (CaO) is an excellent adsorbent because it is inexpensive, robust, and has a high reactivity toward $\rm CO_2$. 18,21 CaO can be obtained from limestone/dolomite by calcination at about 900 °C, 21,22 and it is able to capture CO₂ by a process called carbonation, as shown in eq 1. The CaO carbonation involves an initial fast phase that is kinetically controlled, followed by a second slow phase that is controlled by diffusion. 18,21 Despite the excellent properties of CaO as a solid adsorbent for CO₂ capture, its use presents some drawbacks, as its energyintensive regeneration often results in excessive sintering and mechanical failure. Also, the carbonation process becomes slow after forming the first layers of calcium carbonate. While the capacity of CaO as a sorbent is higher when used as a powder (due to its higher surface area), challenges such as high-pressure drop, entrainment of the flow, and attrition of the material are sometimes observed. 12,21

$$CaO(s) + CO_2(g) \leftrightharpoons CaCO_3(s);$$

 $\Delta H_r^{\circ} = -178.2 \text{ kJ mol}^{-1}$ (1)

Several studies have sought to address the challenges associated with the use of CaO as an adsorbent by improving its stability and reusability using different strategies. For example, Florin et al. investigated the sorption capability of CaO derived from nanosized CaCO₃.²³ The sorbent material was subjected to five cycles of carbonation experiments (24 h/cycle) and they concluded that there was no morphological impediment for the carbonation of CaO derived from nanosized CaCO₃ when giving it enough time. In another

set of experiments, they found that the residual conversion capacity was 20% after 100 CO₂ capture-and-release cycles of 20 min, which is higher than those previously reported for bulk CaO, highlighting the potential of nanosized CaO. Li et al. explored the hydration of CaO with an ethanol-water mixture to help improve the reactivity of the spent adsorbent.²⁴ The authors reported this to improve the sorption capacity of the spent catalyst by twice its initial value. Granados-Pichardo et al. also showed that the sorption capacity of CaO could be enhanced by modifying the synthesis method.²⁵ They synthesized a new CaO-based adsorbent by a fast solution combustion method and a highenergy ball-milling approach. They found that the novel CaO was easily converted to CaCO3 when subjected to a CO2 flow at 25 °C and 1 atm. The high conversion of the asprepared CaO was attributed to the improved textural and structural properties.

To help improve the sorption capabilities of CaO and minimize sintering, Belova et al. adopted the strategy of dispersing CaO on an inert support like γ-Al₂O₃.² previously stated, the carbonation reaction is initially fast, and once a layer of carbonate is formed, this becomes limited by the diffusion of CO2 through that layer. Small CaO particles provide higher surface area and reduced diffusion limitations, and increased dispersion helps to minimize sintering. Similarly, Gruene et al. demonstrated that CaO dispersed on high surface γ-Al₂O₃ resulted in a stable sorbent able to overcome the challenges associated with limited long-term stability, slow uptake kinetics, and energy intensive regeneration.²¹ In this work, CO₂ uptake kinetics and capacities were investigated using thermogravimetric analysis (TGA), while the long-term stability was evaluated through multicycle experiments. They observed that dispersed CaO was an active sorbent at low temperature, with a capacity to bind CO₂ at 300 °C up to 1.7 times when compared to bulk CaO powder. The stability test involved 84 CO₂ capture-andrelease cycles at 650 °C, and this showed that CaO dispersed on γ-Al₂O₃ possessed superior long-term stability than bulk CaO. They also reported that while the adsorption capacity of bulk CaO dropped below 50% after 20 cycles, that was not the case with CaO/γ -Al₂O₃, which after 20 cycles, maintained 90% of its adsorption efficiency with no sintering observed.

Antzara et al. developed a mixed CaO-based CO2 sorbent with inert structural promoters via the sol-gel autocombustion method in an attempt to enhance the resistivity of CaO toward sintering. They found that the most stable sorbents were those containing Al₂O₃ and ZrO₂ as promoters, and they attributed this to the formation of mixed phases of Ca₃Al₂O₆ and CaZrO₃. However, others like Mg-CaO and La-CaO showed lower adsorption capacities and stability than the parent CaO. Guo et al. synthesized a novel Ce-Mn doped calcium-based sorbent and investigated the effect of the incorporation of Ce and Mn on the CO₂ capture.²⁸ The capture cycles were carried out in a thermogravimetric analyzer by monitoring the change of mass with time and temperature. Figure 1 shows the CO₂ uptake of the Ce-Mn doped calcium-based sorbent in comparison with the Cedoped, Mn-doped, and bulk CaO materials. While the CO2 adsorption capacity of the Mn-doped sample decreased continuously with the number of cycles, the Ce-doped sorbent showed a slight increase in the CO₂ uptake, which became constant after ~20 cycles. The self-reactivation in the latter was attributed to structural rearrangement of the

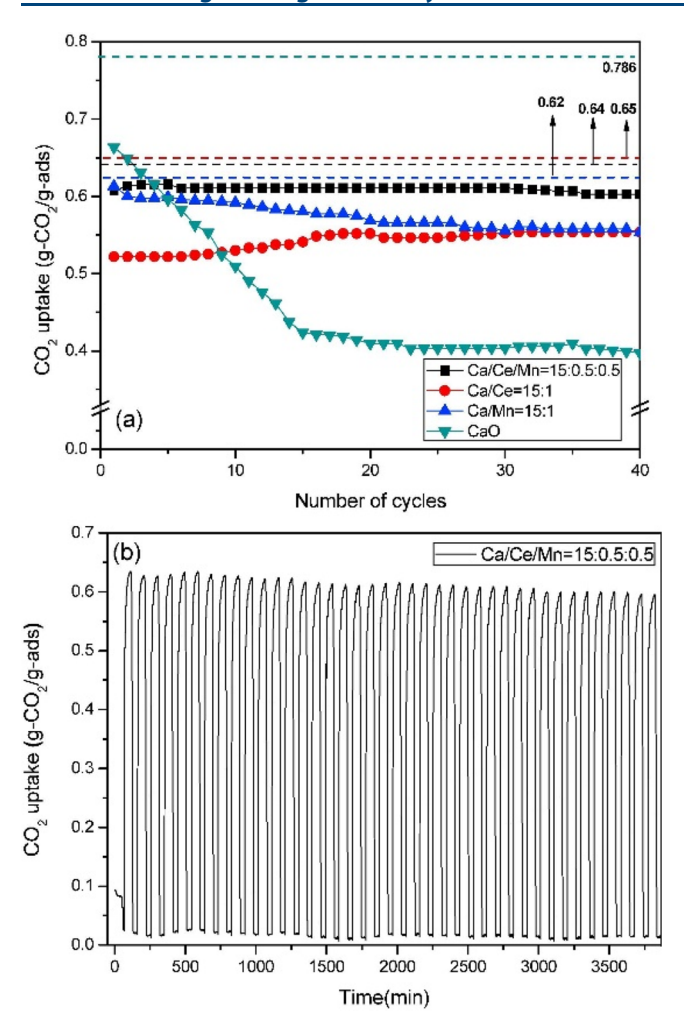


Figure 1. CO_2 uptakes with different synthesized adsorbents as a function of (top) number of cycles and (bottom) carbonation time. Reprinted with permission from ref 28. Copyright 2018 Elsevier.

particles and good dispersion of the inert materials among the CaO particles. The Ce–Mn doped CaO sorbent provided the highest adsorption capacity and stability (0.61 g CO_2/g ads. after 40 cycles). The outstanding performance was attributed to the synergistic interaction between Ce and Mn, the formation of CeO_2 and Ca_2MnO_4 crystallite phases that act as barriers between CaO preventing growth and agglomeration, enhanced dispersion and porosity, and optimized pore size distribution for CO_2 adsorption.

Al-Mamoori also doped CaO in order to improve the adsorption performance.²⁹ In this case, they chose Fe and Ga as the doping metals, and these were incorporated by wet impregnation of their nitrate precursors. They obtained the

highest adsorption capacities of 13.7 mmol/g and 14.2 mmol/g when doping CaO with 10 wt % Fe and 10 wt % Ga, respectively, which was two times better than that of the undoped CaO. Additionally, cyclic adsorption and desorption demonstrated the stability of the doped materials, which retained 95% of their initial capacity after 10 cycles. Table 2 summarizes the adsorbents discussed above and the different strategies used to boost the sorption capacity of CaO.

The CO_2 adsorption capacities of other oxides have also been explored. Yoshikawa et al. investigated the possibility of using single metal oxides to capture CO_2 from flue gas.³⁰ In this work, they explored and compared the sorption capabilities of SiO_2 , Al_2O_3 , ZrO_2 , and CeO_2 with different morphologies: high surface area mesoporous CeO_2 (CeO_2 -1), CeO_2 nanoparticles (CeO_2 -2), and CeO_2 powder (CeO_2 -3) (Figure 2). While SiO_2 showed no CO_2 adsorption, CeO_2 -3 exhibited the most significant CO_2 sorption per weight of sample.

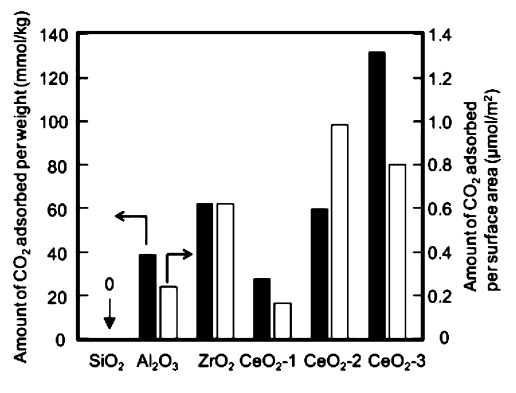


Figure 2. CO_2 adsorbed by different metal oxides as a function of weight and surface area. Reprinted with permission from ref 30. Copyright 2014 Elsevier.

3.2. Carbonate-Based Adsorbents. Carbonates are excellent adsorbents because of their high reactivity toward CO₂, low energy demand, low cost, and the advantage that they do not corrode devices. Liang et al. studied the sorption capacity of Na₂CO₃ in a simulated flue gas.³¹ Equations 2 and 3 show the most important reactions that happen between CO₂ and Na₂CO₃.³¹ They found that Na₂CO₃ captured 90% of CO₂ from flue gas and that there was little or no decrease in the carbonation rate and sorbent capacity after limited multicycle tests.

$$Na_2CO_3(s) + CO_2(g) + H_2O(g) = 2NaHCO_3(s);$$

 $\Delta H_r^{\circ} = -135 \text{ kJ mol}^{-1}$ (2)

Table 2. CaO-Based Adsorbents Showing Different Improvement Strategies, Feeds, and Sorption Capacities

adsorbent	improvement strategy	feed gas composition	temp (°C)	adsorption/desorption cycles	CO_2 sorption capacity(mmol/g)
CaO ²³	increasing the surface area	15% CO ₂ /N ₂	650	5	
CaO ²⁴	hydration with ethanol-water mixture	$15\% \text{ CO}_2/\text{N}_2$	650-700	15	
CaO ²⁵	change of synthesis approach	CO_2	25		9.31
CaO ²⁶	CaO on γ-Al ₂ O ₃ support	$50\% \text{ CO}_2/\text{N}_2$	650	30	
CaO ²¹	dispersing CaO on γ-Al ₂ O ₃ support	$15\% \text{ CO}_2/\text{N}_2$	650	84	6.4
CaO ²⁹	use of dopants like Fe and Ga	$10\% \text{ CO}_2/\text{N}_2$	650	10	13.7-14.1
CaO ²⁸	use of dopant like Ce-Mn	CO_2/N_2	600	40	13.68

Table 3. Carbonate-Based Adsorbents Showing Different Improvement Strategies, Feeds, and Sorption Capacities

adsorbent	improvement strategy	feed gas composition	temp (°C)	adsorption/desorption cycles	CO_2 sorption capacity $(mmol/g)$
$Na_2CO_3^{32}$	Fecralloy coating	10% CO ₂ /Ar	150	500	7.7
$Na_2CO_3^{33}$	amine modification	H_2O/CO_2 (1:1)	50	10	2.51
$K_2CO_3^{34}$	hexagonal crystal structure	10% CO ₂ and 10% H ₂ O	65		
$K_2CO_3^{35}$	K ₂ CO ₃ impregnated on Al ₂ O ₃ support	13% CO ₂ , 13% H ₂ O and 74% N ₂	60-350	10	
$K_{2}CO_{3}^{36}$	K ₂ CO ₃ impregnated on ZrO ₂	9% H ₂ O/1% CO ₂	60-150		1.89-2.11
$K_2CO_3^{8}$	K_2CO_3/γ - Al_2O_3 modified with $Ca(OH)_2$	10% CO ₂ , 12% H ₂ O, 0.05% SO ₂ and 77.95% N ₂	60	25	2.05

$$Na_2CO_3(s) + 0.6CO_2(g) + 0.6H_2O(g)$$

 $\Leftrightarrow 0.4[Na_2CO_3 \cdot 3NaHCO_3](s); \quad \Delta H_r^{\circ} = -82 \text{ kJ mol}^{-1}$
(3)

As the carbonation process is exothermic, a mechanism needs to be put in place to dissipate the heat to allow for continuous adsorption and desorption. One of the strategies to overcome the heat transfer issues is to deposit the sorbent onto metal foils. For example, Kondakindi et al. coated Fecralloy foil, high temperature steel that is an alloy of iron and nickel, with Na₂CO₃/γ-Al₂O₃ and K₂CO₃/γ-Al₂O₃ and compared their CO₂ sorption capacities with those of their powder analogues.³² They discovered that 35 wt % Na₂CO₃/ γ-Al₂O₃ coated on Fecralloy performed much better than its powdery form. Some durability tests were carried out with various foil samples, and they observed a loss of 15% of their capacity through the first 15-20 cycles and 40-50% after 500 cycles. However, they concluded that even after 500 cycles, the Na₂CO₃/ γ -Al₂O₃-coated foil provided a CO₂ capture performance that could be economically competitive with current methods. In an effort to improve the CO₂ sorption capacity of Na2CO3, Yu et al. developed a novel sodium-based adsorbent with amine modification (NaN) that was synthesized using Na₂CO₃, 3-aminopropyltriethoxysilane (APTES), and tetraethylorthosilicate (TEOS) through a solgel approach.³³ They reported that the new material possessed a high sorption capacity of 2.51 mmol/g. In addition, this material was shown to be regenerable and stable during 10 cyclic operations.

K₂CO₃-based adsorbents have also been studied for their capacity to capture CO2 from flue gas. Interestingly, Zhao et al. studied the effect of the crystal structure on the capacity to adsorb CO₂.³⁴ Given that the carbonation reactivity of the monoclinic crystal K2CO3 was much less than that of the hexagonal crystal, they concluded that the crystal structure had an important effect on the CO2 adsorption capacity. Zhao et al. also prepared a K₂CO₃-based adsorbent by impregnating K₂CO₃ on Al₂O₃. This material was tested in a bubbling fluidized-bed reactor, and they found that the CO₂-capture capacity of K₂CO₃/Al₂O₃ was above 90% during 10 cycles and that there were little morphological changes in the sorbent after the cyclic studies. Lee et al. studied the thermal stability of K₂CO₃ sorbent when deposited onto ZrO2 and TiO2 supports to be used in a fixed bed reactor within a temperature range of 60-150 °C.³⁶ They found that when K₂CO₃/TiO₂ was calcined in air (or N₂) at temperatures over 500 °C, the CO₂ capture capacity decreased rapidly. This was attributed to the generation of K₂Ti₂O₅ and K₂Ti₆O₁₃ inactive species during calcination. However, the K₂CO₃/ZrO₂ sample displayed a CO₂ capture capacity of about 83-93 mg CO₂/g sorbent despite the

calcination at temperatures in the range of 500–700 $^{\circ}$ C. They concluded that this was the result of the ability of $K_2\text{CO}_3$ and $Z\text{rO}_2$ to maintain their phases without forming any new alloy species.

Wu et al. studied the failure mechanism of potassium-based sorbents (K₂CO₃ and K₂CO₃/Al₂O₃) when capturing CO₂ from a simulated flue gas containing 500 ppm of SO₂. From X-ray diffraction (XRD) studies, they observed the formation of KHCO₃ and K₂SO₃, which is undesirable because the generation of K₂SO₃ reduces the utilization ratio of the sorbent. They also observed that the presence of water accelerated the sulfation reaction of K₂CO₂. However, the K₂CO₃/Al₂O₃ supported sorbent material showed good carbonation and antisulfation properties after pretreatment with water, which can slow the failure of the sorbent. To increase the CO₂ sorption capacity of supported K₂CO₃ and reduce its consumption due to the presence of SO2 in real flue gas, Wu et al. also synthesized inexpensive calcium-modified K_2CO_3 sorbents.³⁸ They explored the addition of three calcium additives, Ca(OH)2, CaO, and CaCO3, to K₂CO₃/γ-Al₂O₃ for CO₂ capture under simulated flue gas condition, and concluded that Ca(OH)2 was the most effective one. Remarkably, the Ca(OH)₂-modified K₂CO₃/γ-Al₂O₃ material not only showed a higher CO₂ sorption capacity but also proved to be more robust under SO₂containing flue gas than the unmodified $K_2CO_3/\gamma-Al_2O_3$ sample. A summary of some of the carbonate-based adsorbents reported in the literature is shown in Table 3.

This section discussed several strategies adopted to improve the sorption capacity of both oxides and carbonate-based adsorbents. However, further investigation is needed to make them cost-effective and suitable for large-scale operations. The use of these adsorbents together with catalytic materials to synthesize dual-function materials for capture and conversion of CO_2 into value-added products is reviewed in the following sections.

4. DUAL-FUNCTION MATERIALS

Dual-function materials (DFMs) are materials composed of a sorbent and a catalytic active component. The oxides and carbonates previously discussed typically serve as the CO₂ adsorbent, while metal species catalyze the conversion of adsorbed CO₂. Melo Bravo and Debecker recently reviewed the use of DFMs for combined CO₂ capture and catalytic conversion to methane.³⁹ These DFMs, comprised of both basicity and redox catalytic sites, allow for in situ CO₂ capture and conversion via a process often referred to as CO₂ capture-reduction (CCR). These systems involve the sequential feeding and intermittent switching between different gas streams. Diluted CO₂ streams are first fed until complete saturation of the adsorbent species (carbo-

Table 4. Ni-Based DFMs: Synthesis Methods and Relevant Reaction Conditions

			temp	(°C)	feed composition	
DFM	synthesis method	reaction ^a	adsorption	reaction	adsorption	reaction
Ni-CaO ⁶⁰	Pechini sol-gel	DRM	600	800	CO_2	CH ₄
CaO + Ni/MgO-Al ₂ O ₃ ⁶¹	coprecipitation	DRM	720	720	$20\% \text{ CO}_2/\text{N}_2$	2.4% CH ₄ /N ₂
Ni-CaO-Ce ⁶²	sol-gel combustion	RWGS	650-750	650-750	15% CO ₂ /N ₂	$5\% H_2/N_2$
$Ni-(K-Ca)/\gamma-Al_2O_3^2$	wet impregnation	DER	650	650	$10\% \text{ CO}_2/\text{N}_2$	$5\% C_2H_6/N_2$
$Ni-(Na-Ca)/\gamma-Al_2O_3^2$	wet impregnation	DER	650	650	$10\% \text{ CO}_2/\text{N}_2$	$5\% C_2H_6/N_2$
$Ni-(K-Mg)/\gamma-Al_2O_3^2$	wet impregnation	DER	650	650	$10\% \text{ CO}_2/\text{N}_2$	$5\% C_2H_6/N_2$
$Ni-(Na-Mg)/\gamma-Al_2O_3^2$	wet impregnation	DER	650	650	$10\% \text{ CO}_2/\text{N}_2$	$5\% C_2H_6/N_2$
Ni-CaO/Al ₂ O ₃ ⁶³	wet impregnation	methanation	280-520	280-520	10% CO ₂ /Ar	10% H ₂ /Ar
$Ni-Na_2CO_3/Al_2O_3^{63}$	wet impregnation	methanation	280-520	280-520	10% CO ₂ /Ar	10% H ₂ /Ar
$Ni-Na_2O/Al_2O_3^{64}$	incipient wetness impregnation	methanation	320	320	7.5% CO_2/N_2 and 7.5% CO_2 , 4.5% O_2 , 15% H_2O/N_2	$15\% \ H_2/N_2$

"Notation: DRM: Dry reforming of methane, DER: Dry ethane reforming, and RWGS: reverse water-gas shift.

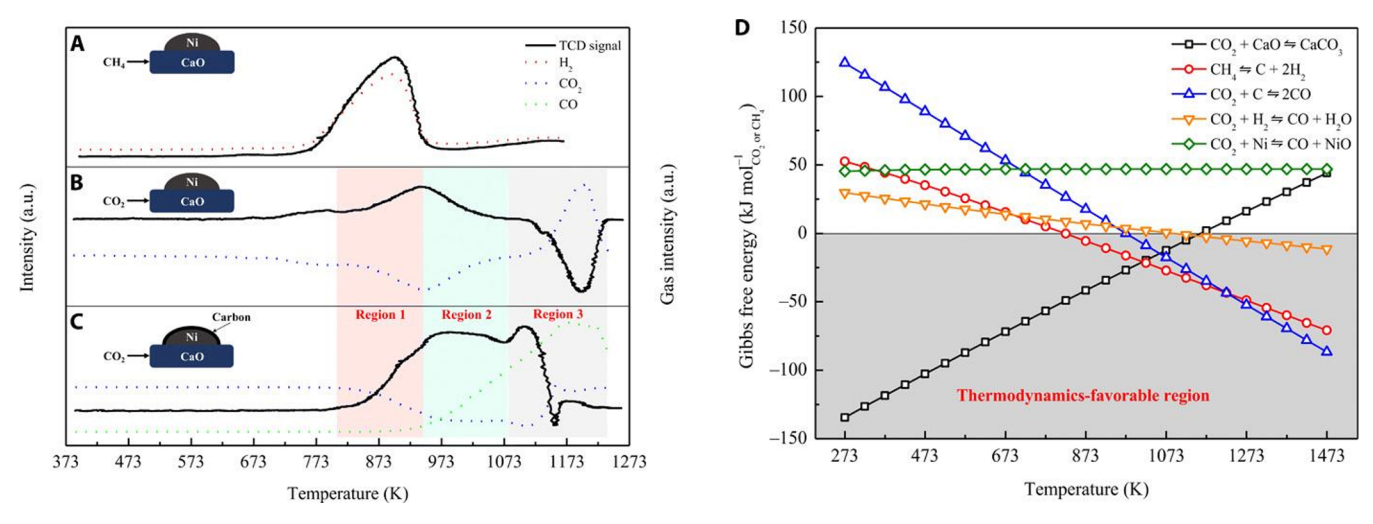


Figure 3. Temperature-programmed surface reactions on a CaO-Ni DFM to identify the reactions involved in the process (A–C) and Gibbs free energy of the different reactions involved as a function of the temperature (D). Reprinted with permission from ref 60. Copyright 2019 American Association for the Advancement of Science.

nation or weak chemisorption). Then, a reactive component such as H₂ or CH₄/C₂H₆ (as in reforming reactions) is flowed to convert adsorbed CO2. This strategy eliminates the CO₂ transportation and storage challenges associated with CCS processes. Furthermore, the in situ capture and conversion of CO2 on DFMs eliminates the high-energy penalty associated with the thermal swing regeneration process prevalent in other postcombustion capture schemes, such as amine scrubbing. It is also worth mentioning that both the chemisorption and physisorption properties of sorbents could affect the working capacity of DFMs. While the physisorption is associated with the occurrence of van der Waals forces and a low heat of adsorption,⁴⁰ in the chemisorption, CO₂ undergoes a covalent chemical reaction with the sorbent sites and incurs a much greater heat of adsorption. Physisorption processes are less selective, leading to the adsorption of other gases such as N2 that lowers the purity of the adsorbed CO2; however, chemisorption could lead to the permanent binding of poisons, such as SO2, hence decreasing the capacity of the sorbents. Nevertheless, the predominant chemisorption process in DFMs allows for higher affinity to CO2 in diluted streams. Parameters such as the weight loading of sorbent and catalytic species, ratio of sorbent to catalyst, temperature of adsorption and reaction, and composition of the feed gas streams are important in the

design of DFMs, as they are essential in the optimization of the sorption capacity, reactive potential, and stability. In this section, we critically review and discuss different DFMs developed for CO_2 capture and conversion.

4.1. Ni-Based DFMs. Nickel has been recurrently used for CO_2 conversion reactions, such as methanation, $^{41-47}$ reverse water-gas shift (RWGS), $^{48-52}$ and reforming of methane and other light alkanes. In addition to its high activity, its frequency of utilization comes from the fact that it is highly abundant and less expensive than other metals. Owing to its classical use for CO_2 reactions, it has become a primary target for the synthesis of DFMs. Table 4 compiles some examples of Ni-based DFMs indicating the synthesis method, reaction used, and main reaction parameters.

Tian et al. carried out a calcium-looping methane reforming process using a CaO-Ni bifunctional sorbent-catalyst prepared via the Pechini sol—gel method. The synthesis involved the dissolution of calcium and nickel nitrates together with anhydrous citric acid in water with stirring at 75 °C. Next, after addition of ethylene glycol, the temperature of the solution was raised to 90 °C to induce gelation. The resultant gel was dried overnight at 100 °C and calcined at 800 °C for 2 h to obtain the CaO–Ni sorbent-catalyst. First, CO₂ is captured by reacting with CaO adsorbent to form CaCO₃ (eq 1), then this is decomposed

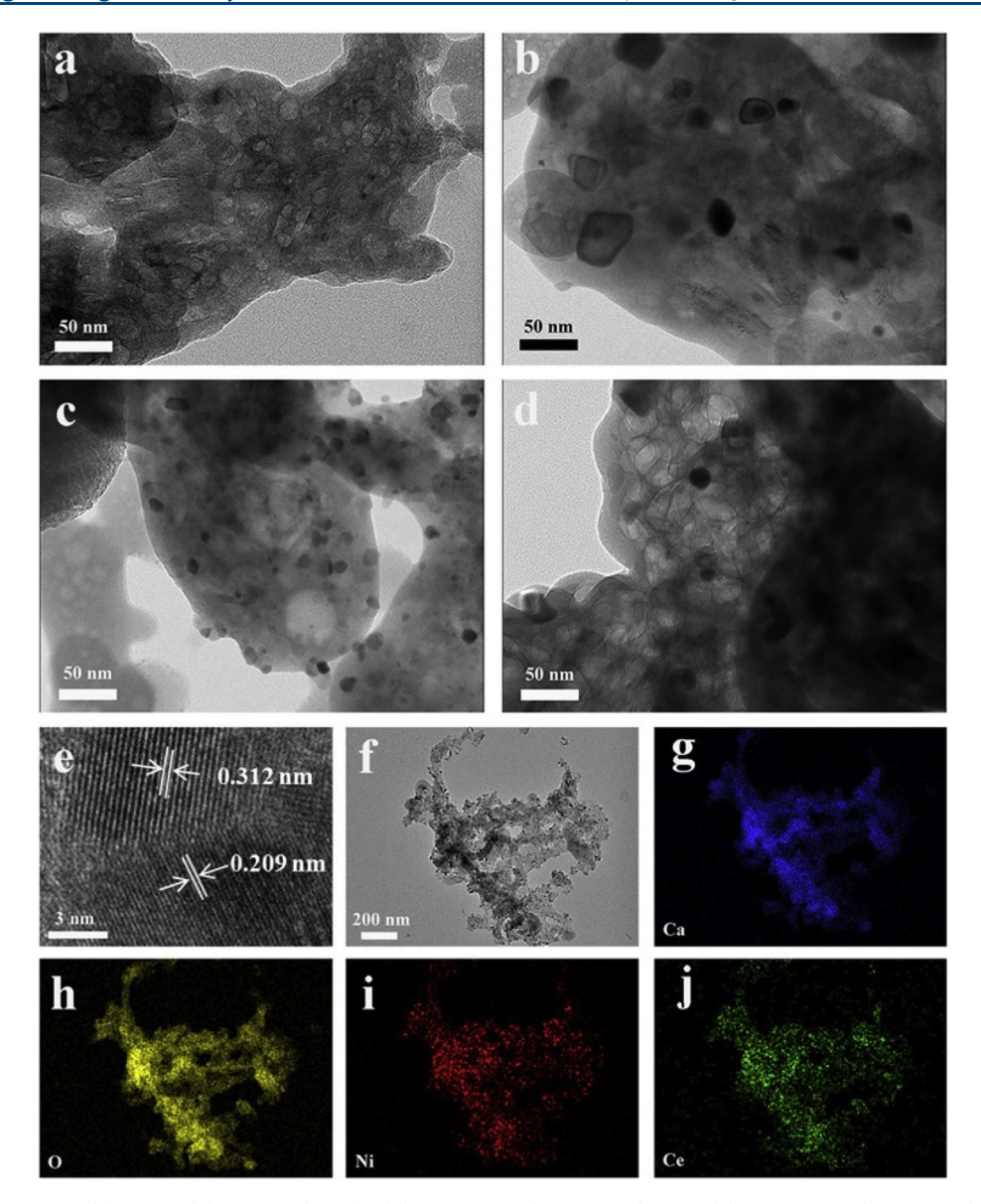


Figure 4. TEM images of (a) CaO, (b) Ca/Ni (1:0.1), (c) Ca/Ni/Ce (1:0.1:0.017), and (d) Ca/Ni/Ce (1:0.1:0.033). HRTEM (e) and elemental mappings (f-i) of Ca/Ni/Ce (1:0.1:0.033). All in molar ratio. Reprinted with permission from ref 62. Copyright 2019 Elsevier.

to bring CO_2 to the CaO-Ni interface for the reaction with CH_4 (dry reforming) to produce syngas according to eq 4.

$$CO_2(g) + CH_4(g) = 2CO(g) + 2H_2(g);$$

 $\Delta H_r^{\circ} = +247.0 \text{ kJ mol}^{-1}$ (4)

Although the CO_2 adsorption experiments were performed at 600 °C, methane reforming took place at 800 °C, indicating a nonisothermal capture and conversion process. This is due to the fact that both the CO_2 desorption and methane reforming reaction are endothermic. The purported reaction mechanism elucidated by temperature-programmed surface reaction (TPSR) studies revealed the decomposition of CaCO_3 to CO_2 under methanation conditions, and the dissociation of CH_4 on the Ni surface (Figure 3). This eventually led to the reverse Boudouard reaction between CO_2 and the carbon deposited on the $\mathrm{CaO-Ni}$ interface to produce CO . It was observed that the carbon deposited onto the $\mathrm{CaO-Ni}$ DFM led to a more facile CO_2 consumption, as the thermodynamics of the reverse Boudouard reaction was

more favorable (Figure 3D). This process resulted in 65% CO₂ utilization efficiency and 86% CH₄ conversion, which makes it competitive when compared to other novel methane reforming processes. They concluded that the in situ consumption of CO₂ on the catalyst surface during methane dry reforming shifted the equilibrium to the right favoring the dissociation of CaCO₃ according to Le Chatelier's principle. This allowed the otherwise energy-intensive calcium looping process to be operated at lower temperatures, thus mitigating a major issue of deactivation through sintering. This system was found to be highly energy efficient, with the energy consumed during the CO₂ utilization being 22% lower than that of conventional methane dry reforming.

Kim et al. also conducted the dry reforming of methane with a Ni-based catalyst (Ni/MgO–Al $_2$ O $_3$) containing a CaO sorbent. As in the previous work, they also used a calcium looping process to capture and convert CO $_2$. Precalcined limestone was mixed with the Ni catalyst and was subjected to high-temperature calcination and reduction treatments at 800 °C. The temperature was then reduced to 720 °C for the

carbonation experiments with 20 vol % $\rm CO_2$ in $\rm N_2$. Unlike the report by Tian et al., 60 both the $\rm CO_2$ carbonation—desorption and subsequent methane reforming were conducted isothermally (720 °C) with 2.4 vol % $\rm CH_4$ in $\rm N_2$ to produce synthesis gas. Although the process operated efficiently over 10 cyclic experiments, deactivation was observed by sintering of the CaO sorbent.

Other researchers have explored means for modifying the sorbent species to improve the CO2 capture and the conversion process on Ni-based DFMs. For example, Sun et al. studied the use of a Ce-modified CaO adsorbent for the development of Ni-based DFMs. 62 These DFMs were synthesized via a sol-gel combustion method using calcium and nickel nitrate precursors and citric acid as a chelating agent. For the preparation of Ce-doped DFMs, a cerium nitrate precursor was introduced into the synthesis mixture with a Ce2+ to Ca2+ molar ratio of 1:30 and 1:60, and the morphology and elemental mapping of the as-synthesized DFMs are shown in Figure 4. Integrated CO₂ capture and conversion experiments were carried out at 650 °C using 15% CO₂/N₂ and 5% H₂/N₂, respectively, with pristine CaO, Ni-CaO, and Ce-modified Ni-CaO systems. These materials were studied in the reverse water-gas shift (RWGS) reaction shown in eq 5.

$$CO_2(g) + H_2(g) \leftrightharpoons CO(g) + H_2O(g);$$

$$\Delta H_r^{\circ} = +41.2 \text{ kJ mol}^{-1}$$
(5)

Even though the bare CaO had the highest CO2 capture capacity of 15.7 mmol/g, the CO₂ conversion was only 23.4%. However, adding Ni to CaO (Ca/Ni molar ratio of 1:0.1) led to a 46% CO₂ conversion. Additional incorporation of the Ce promoter (Ca/Ni/Ce molar ratio of 1:0.1:0.017) improved the conversion to 50.7%, while a further increase in the cerium loading (Ca/Ni/Ce molar ratio of 1:0.1:0.033) led to an improved activity with 51.8% CO2 conversion and nearly 100% CO selectivity. As expected, increasing the reaction temperature from 650 °C to 700 and 750 °C using the Ca/Ni/Ce (1:0.1:0.033) sample increased the rate of CaCO₂ decomposition; however, there was a negligible increase in the rate of the RWGS reaction, indicating that 650 °C was the optimum temperature for carbon capture and conversion to CO. At 650 °C, this DFM also showed to be stable after 20 cycles of integrated capture and conversion of CO2, while the unmodified Ni-CaO system (no Ce) exhibited a rapid drop off in activity with increasing cycles. It was concluded that the introduction of cerium oxide into the material resulted in a more facile reduction of the dissociated CO2 regenerated from the DMF (owing to the presence of oxygen vacancies) and the homogeneous dispersion of CeO2 over the DFM acted as a physical barrier preventing the sintering of CaO and NiO species, as it can be seen in Figure 4c.

The authors also discussed the potential reaction pathways over DFMs. So far, two possible mechanisms have been proposed in the literature for the RWGS reaction: redox mechanism (scheme 1 in Figure 5) and the associative "formate" mechanism (scheme 2 in Figure 5). On the basis of in situ DRIFTS spectra, they concluded that both mechanisms coexist; however, owing to the similarities of the DRIFTS spectra for all DFMs, they concluded that surface formate and carbonyl were not the main reaction intermediates that cause the differences in performance. For

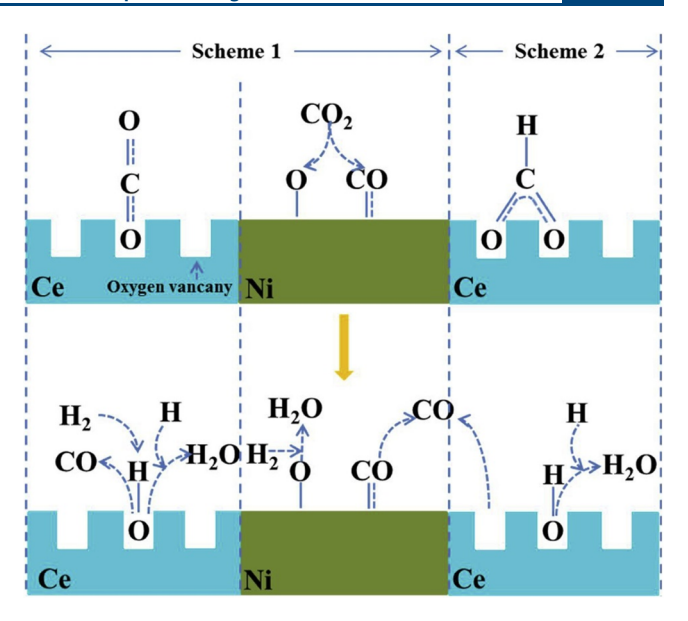


Figure 5. RWGS reaction mechanisms over DFMs. Reprinted with permission from ref 62. Copyright 2019 Elsevier.

the Ni–CaO system, it was suggested that upon switching the gas to H_2 , CO_2 spills over and reacts with Ni active sites producing CO and NiO (eq 6), and NiO species are reduced by the adsorbed H_2 as shown in eq 7. However, when the DFM is doped with cerium, CO_2 interacts over an oxygen vacancy (Ce^{3+}) resulting in the oxidation to Ce^{4+} and release of a CO molecule (eq 10). Then, adsorbed H_2 species extract lattice oxygen from ceria producing H_2O and the reduction of the catalyst back to Ce^{3+} (eq 9).

$$CO_2 + Ni = CO + Ni^{2+}$$
 (6)

$$H_2 + Ni^{2+} \rightleftharpoons H_2O + Ni \tag{7}$$

$$CO_2 + Ce^{3+} = CO + Ce^{4+}$$
 (8)

$$H_2 + Ce^{4+} = H_2O + Ce^{3+}$$
 (9)

Al-Mamoori et al. reported the use of Ni-impregnated CaO- and MgO-based double salts supported on γ -Al₂O₃ as DFMs for CO₂ capture and conversion to syngas via dry ethane reforming according to eq 10. 65

$$2CO_2 + C_2H_6 = 4CO + 3H_2;$$

 $\Delta H_r^{\circ} = +428.1 \text{ kJ mol}^{-1}$ (10)

First, they impregnated different double salts based on K-and Na-promoted CaO and MgO (K–Ca, Na–Ca, K–Mg, and Na–Mg) on γ -Al₂O₃. After drying and calcination, the materials were impregnated again with Ni(NO₃)₂·6H₂O to obtain the desired DFMs. For the CO₂ capture and conversion experiments, a 10% CO₂/N₂ mixture was fed at 650 °C and 1 bar until saturation before switching to 5% C₂H₆/N₂ at the same temperature. The Ni@(K–Ca)/ γ -Al₂O₃ system showed the best CO₂ adsorption and desorption capacities, being 0.99 and 0.95 mmol/g, respectively, while displaying a 100% C₂H₆ conversion and 65% of CO₂ reacted to form syngas. Even when the high Ni loading contributed to the formation of coke due to cracking reactions, the catalyst showed long-term stability with only a 5% drop in the catalytic activity after 600 min.

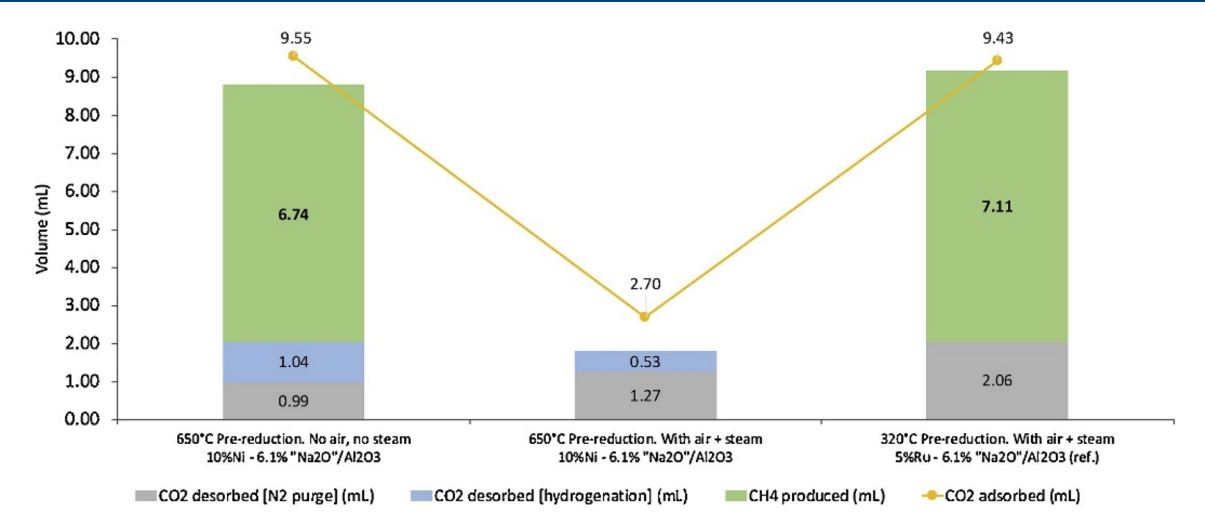


Figure 6. CO₂ capture capacity and methanation activity over Ni- and Ru-based DFMs. Reprinted with permission from ref 64. Copyright 2019, Elsevier.

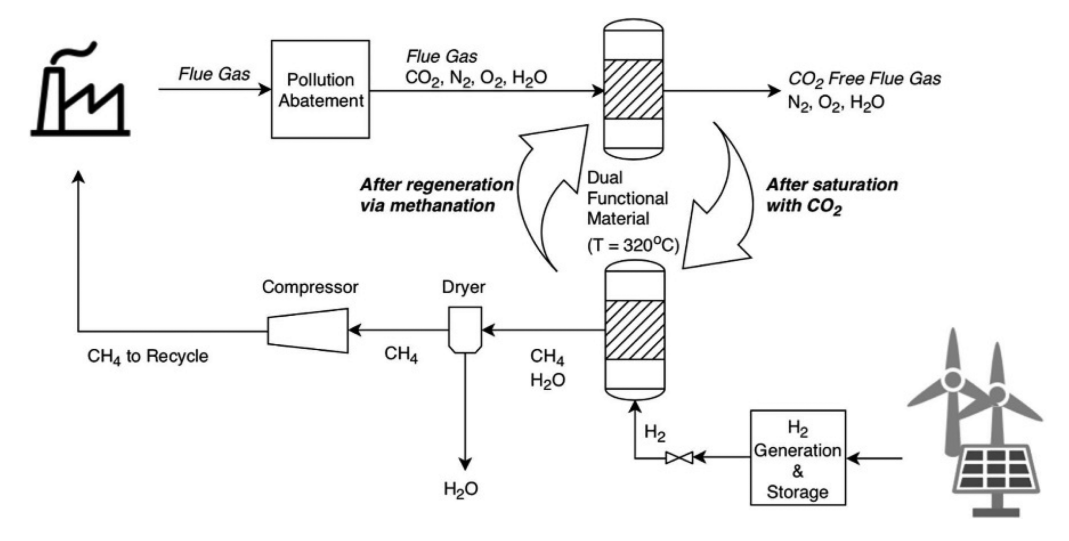


Figure 7. Proposed process flow diagram for the use of DFMs for CO₂ capture and methanation. Reprinted with permission from ref 66. Copyright 2019 Elsevier.

Bermejo-López et al. studied the effect of the Ni loading on the capture and in situ conversion of CO₂ to CH₄ (methanation) using CaO and Na₂CO₃ as sorbents (eq 11).

$$CO_2 + 4H_2 \leftrightharpoons CH_4 + 2H_2O; \quad \Delta H_r^{\circ} = -165.0 \text{ kJ mol}^{-1}$$
(11)

Several Ni-CaO/ γ -Al₂O₃ and Ni-Na₂CO₃/ γ -Al₂O₃ DFMs with different Ni loadings were synthesized via wetness impregnation. These materials were used for CO₂ capture and conversion using 10% CO₂/Ar and 10% H₂/Ar gas streams for capture and hydrogenation, respectively. It was observed that the Ni reducibility was improved at high Ni loadings and when these adsorbents were incorporated. Kinetic studies revealed that the production of methane increased with the Ni loading until reaching a value of 142 μ mol/g with the 15% Ni-15% CaO/ γ -Al₂O₃ sample at 520 °C. However, even better results were obtained with the samples containing Na₂CO₃, being this of 186 μ mol/g when using the 10% Ni-10% Na₂CO₃/Al₂O₃ sample even at a lower temperature (400 °C).

In the same year, Arellano-Treviño et al. described some limitations of the Ni-based DFMs for production of methane

in simulated flue gas applications.⁶⁴ The sorbent species were first deposited on the γ-Al₂O₃ support via incipient wetness impregnation. After drying and calcination in air, the catalyst precursor was impregnated to obtain the DFM. The asprepared Ni-Na₂O/Al₂O₃ DFM was subjected to CO₂ capture using 7.5% CO₂/N₂ and a simulated flue gas (7.5% CO₂, 4.5% O₂, 15% H₂O, balance N₂) at 320 °C and atmospheric pressure. In the first case (ideal 7.5% CO_2/N_2), the Ni-based DFM yielded a CO2 capture capacity of 9.55 mL, a high capacity that was attributed to both the presence of the Na₂O/Al₂O₃ adsorbent and Ni being fully reduced and active toward CO₂ adsorption. As it can be seen in Figure 6, its further hydrogenation produced 6.74 mL of CH₄. However, when using the simulated flue gas, the activity dropped dramatically with only 2.70 mL of CO₂ captured and no methane formation. For comparison purposes, a reference Ru-based DFM sample prereduced at 320 °C and subjected to the same simulated flue gas yielded a CO2 capture capacity of 9.43 mL and produced 7.11 mL of methane upon hydrogenation (Figure 6). The low CO₂ capture capacity and null methanation activity of the Nibased DFM under simulated flue gas conditions was ascribed

Table 5. Ru and Rh-Based DFMs: Synthesis Methods and Relevant Reaction Conditions

			temp (°C)		feed composition	
DFM	synthesis method	reaction	adsorption	reaction	adsorption	reaction
$\text{Ru-CaO}/\gamma\text{-Al}_2\text{O}_3^{74}$	incipient wetness impregnation	methanation	320	320	$10\%\ CO_2/air$ and $8\%\ CO_2/21\%\ H_2O/air$	5% H ₂ /N ₂
$\text{Ru-CaO}/\gamma\text{-Al}_2\text{O}_3^{14}$	incipient wetness impregnation	methanation	320	320	$10\% \text{ CO}_2/\text{N}_2$	$4\% \ H_2/N_2$
$\text{Ru-CaO}/\gamma\text{-Al}_2\text{O}_3^{70}$	incipient wetness impregnation	methanation	320	320	7.5% CO ₂ , 4.5% O ₂ , 15% H ₂ O/N ₂	5% H ₂ / N ₂
$Ru-Na_2CO_3/\gamma-Al_2O_3^{75}$	incipient wetness impregnation	methanation	320	320	7.5% CO_2/N_2 and 7.5% CO_2 , 4.5% O_2 , 15% H_2O/N_2	5% H ₂ /N ₂
$Ru-Na_2O/\gamma-Al_2O_3^{76}$	incipient wetness impregnation	methanation	250-350	250-350	7.5% CO ₂ , 4.5% O ₂ , 15% H ₂ O/N ₂	$15\% \ H_2/N_2$
Ru-CaO/ γ -Al ₂ O ₃ ⁷⁷	incipient wetness impregnation	methanation	280-400	280-400	1.4% CO ₂ /Ar and 11% CO ₂ /Ar	10% H ₂ /Ar
$Ru-Na_2CO_3/\gamma-Al_2O_3^{77}$	incipient wetness impregnation	methanation	280-400	280-400	1.4% CO ₂ /Ar and 11% CO ₂ /Ar	10% H ₂ /Ar
$Ru-Na_2O/\gamma-Al_2O_3^{14}$	incipient wetness impregnation	methanation	320	320	15% CO ₂ /N ₂	$20\% \ H_2/N_2$
Rh-CaO/ γ -Al ₂ O ₃ ¹⁴	incipient wetness impregnation	methanation	320	320	10% CO ₂ /N ₂	$2\% \ H_2/N_2$

to the oxidation of Ni to NiO during the capture step. It is well-known that Ni catalysts typically require high reduction temperatures and are susceptible to oxygen-containing feeds. With these challenges in mind, the same research group decided to explore the modification of Ni with trace amount of precious metals (≤1 wt % Pt, Pd or Ru) because they are known to dissociate H₂ lowering the reduction temperature.⁶⁶ They observed that the introduction of 1 wt % Pt and Ru improved the reduction of NiO_x to Ni (at 320 °C) by 50% and 70%, respectively, thereby, enhancing the methanation activity in simulated flue gas conditions. The best result was obtained with a 1% Ru, 10% Ni, 6.1% Na₂O/Al₂O₃ DFM system that provided a CO₂ capture capacity of 0.52 mmol CO₂/g and yielded a methane production of 0.38 mmol CH₄/g at 320 °C, which are much higher than those obtained with the 10% Ni, 6.1% Na₂O/Al₂O₃ DFM that provided a CO₂ capture capacity of 0.11 mmol CO₂/g without CH₄ production at 650 °C. Remarkably, this catalyst also proved to be stable for 20 cyclic tests. However, Pd- and Pt-modified Ni-based DFMs generally exhibited much lower hydrogenation and methanation rates. This together with their high cost make them unable to compete with Ru-Ni systems. The presence of Ni in the Ru-Ni system generally improved the CO₂ sorption capacity and increased the amount of methane produced; however, there exists a tradeoff in slower methanation rates. This innovative bimetallic approach involving a blend of precious and base metals could be implemented to enhance the dual functionality for CO2 processes while also reducing their associated costs. These researchers also proposed a layout for incorporating the DFM in close proximity to a power plant and a hydrogen generation unit (Figure 7).66 The schematic shows the pretreatment of flue gas to remove pollutants before feeding it to the DFM unit. Then, captured CO2 is hydrogenated to produce methane, which can be recycled as a fuel source, thereby closing the carbon cycle. The beauty of this operation is that the CO₂ adsorption and methanation can be conducted isothermally, and the synergistic effect of the reaction ensures that the heat released during methanation drives the CO₂ desorption process.

In some instances, the CO₂ capture is performed postreaction. Wu and Williams⁶⁷ developed a Ni-based

DFM (Ni-Mg-Al-CaO), and interestingly, this material was not used for the direct capture of CO2 from diluted or simulated flue gas streams and further conversion, but for the in situ adsorption of CO2 produced during the pyrolysisgasification of polypropylene. The pyrolysis-gasification of polypropylene culminates in the production of H₂ via the water-gas shift (WGS) reaction (CO + $H_2O \rightleftharpoons CO_2 + H_2$), and the removal of CO₂ from the product stream by DFMs permits the obtain hydrogen in higher concentrations. In the presence of the Ni-Mg-Al-CaO DFM, it was observed that the gas yield in terms of weight of polypropylene increased from 68.1 to 252.3 wt % when the gasification temperature increased from 700 to 800 $^{\circ}\text{C}$. Interestingly, when using this DFM, the H_2/CO ratio remained constant at ~ 3 at all temperatures, which was attributed to the in situ removal of CO₂ and consequent promotion of the WGS reaction. This catalyst/sorbent system also proved to be stable after five cycles of carbonation/calcination at 750 °C, while the activity of bare CaO showed an evident decay. Likewise, Di Felice et al. developed Fe and Ni catalysts for biomass gasification with simultaneous CO₂ capture and tar reforming.⁶⁸ Ni and Fe were supported on CaO, MgO, and calcined dolomite, and these materials were studied over a temperature range from 650 to 850 °C. For all metal/substrates systems, it was observed that low metal loadings were as effective as higher loadings for tar abatement purposes, with the Ni-based system being particularly reactive. The challenges associated with this biomass postreaction CO2 capture include carbon deposition and particle attrition. However, the addition of Fe or Ni to the traditional oxide sorbent helped to mitigate the carbon deposition. Likewise, the use of an excess of steam in the biomass gasification system can inhibit the coke formation. Additionally, attrition was minimized due to the strong interaction between metal and support, an important factor for large-scale fluidized bed applications.

Even when Ni is one of the most abundant metals on Earth, its use for the development of DFMs suffers from challenges such as high reduction temperature (typically >600 $^{\circ}$ C) and tendency to deactivate in simulated flue gas conditions. This has motivated others to use other elements, such as Ru and Rh, even when they are costly and less abundant. Nevertheless, it should be noted that Ni-based

DFMs possess great versatility in a broad range of applications, such as in methane synthesis, RWGS, and reforming-based reactions. More in-depth studies are still needed for the development of highly stable Ni-based DFMs, and further emphasis should be put in understanding the mechanisms involved in the $\rm CO_2$ adsorption and conversion on these DFM structures. A better understanding of the reaction pathways could also provide additional insights for the optimization of the process conditions for increased selectivity.

4.2. Ru- and Rh-Based DFMs. Ruthenium has been extensively studied because of its high activity and selectivity in the methanation of CO₂. Ru has gained a lot of traction due to its rapid reversible redox behavior that allows it to easily transition between its metallic and oxide states. These attributes have made this element to be considered as an active replacement for Ni in the development of DFMs despite its high cost. Table 5 compiles some examples of Ru and Rh-based DFMs indicating the synthesis method, reaction used, and main reaction parameters.

Ru-based DFMs have been one of the most studied for capture and conversion of CO₂. Duyar et al. published one of the earliest reports on Ru-based DFMs for CO2 capture and methanation.⁷⁴ In their work, they made use of CaO as the sorbent component and Ru as the catalyst, and both were dispersed onto a γ-Al₂O₃ support. These DFMs were synthesized by conventional incipient wetness impregnation using Ru(NO)(NO₃)₂ and Ca(NO₃)₂ as precursors. First, $Ru(NO)(NO_3)_2$ was impregnated on 10 wt % CaO/γ - Al_2O_3 followed by pretreatment in air at 320 °C for 2 h to decompose the Ru salt, providing this temperature the maximum Ru dispersion. Then, another DFM was synthesized by impregnating Ca(NO₃)₂ on 10 wt % Ru/γ-Al₂O₃, followed by an in situ reduction at 320 °C to decompose Ca(NO₃)₂ into CaO.⁷⁴ To properly study the effectiveness of the DFMs, different weight loadings of Ru catalyst (1-11 wt %) and CaO adsorbent (1-10 wt %) were used. The capture step involved the exposure of the material to a 10% CO₂/N₂ stream at 320 °C, followed by methanation with $4\% H_2/N_2$ for 2 h at the same temperature. It is worth mentioning that the methanation reaction (eq 11) is exothermic, which allows for an efficient heat integration with the CO₂ desorption and spillover to the catalytic sites, making possible the isothermal CO₂ capture and conversion. Optimization studies showed that 5% Ru, 10% CaO/γ-Al₂O₃ was the best DFM, displaying the highest methanation activity of 0.50 g-mol CH₄/kg DFM, a 5-fold improvement when compared to the base 10% Ru/γ-Al₂O₃ material (Table 6). It was also observed that it was more effective to deposit Ru onto CaO/γ-Al₂O₃, and this was attributed to an increased dispersion of Ru on the DFM as compared to the coverage of Ru sites when CaO was impregnated onto Ru/γ - Al_2O_3 . In any case, the incorporation of the CaO sorbent to the Ru catalyst markedly improved the methanation activity of the catalyst, and even a physical mixture of 10% Ru/ γ -Al₂O₃ and 10% CaO/ γ -Al₂O₃ provided better results than pristine 10% Ru/γ-Al₂O₃. This was explained by spillover of CO2 from the CaO sites to Ru sites during the hydrogenation stage. The mechanism of the spillover process on the Ru-CaO/γ-Al₂O₃ DFM is shown in eqs 12-15. The 5% Ru, 10% CaO/ γ -Al₂O₃ DFM also proved to be highly stable under accelerated aging conditions

Table 6. Methane Turnover (mol CH₄ Produced/mol Ru Present in Sample) and Methanation Capacity Reported over Different Ru-based DFMs. Reprinted with permission from ref 74. Copyright 2015 Elsevier

sample	CH ₄ /Ru	g-mol CH ₄ /kg DFM
γ -Al ₂ O ₃	0	0.00
10% Ru/ γ -Al ₂ O ₃	0.1	0.10
1% CaO, 10% Ru/γ - Al_2O_3	0.19	0.19
5% CaO, 10% Ru/γ-Al ₂ O ₃	0.27	0.27
10% CaO, 10% Ru/γ-Al ₂ O ₃	0.31	0.30
1.1% Ru, 10% CaO/γ-Al ₂ O ₃	2.46	0.27
2% Ru, 10% CaO/γ - Al_2O_3	1.79	0.35
5% Ru, 10% CaO/γ - Al_2O_3	1.01	0.50
6.8% Ru, 10% CaO/γ-Al ₂ O ₃	0.65	0.44
10.6% Ru, 10% CaO/γ-Al ₂ O ₃	0.44	0.46
10% Ru/ γ -Al ₂ O ₃ + 10% CaO/ γ -Al ₂ O ₃	0.25	0.12

using an 8% CO₂/21% H₂O/air feed after 20 cycles on stream (Figure 8).

CO₂ adsorption onto CaO sites:

$$CO_2 + CaO/\gamma - Al_2O_3 \rightarrow CO_2 \cdots CaO/\gamma - Al_2O_3$$
 (12)

CO₂ spillover from CaO sites and adsorption on Ru sites:

$$CO_2 \cdots CaO/\gamma - Al_2O_3 \rightarrow CO_2 + CaO/\gamma - Al_2O_3$$
 (13)

$$CO_2 + Ru/\gamma - Al_2O_3 \rightarrow CO_2 \cdots Ru/\gamma - Al_2O_3$$
 (14)

CO₂ methanation on Ru sites when exposed to H₂:

$$CO_2 + 4H_2 \rightarrow CH_4 + 2H_2O$$
 (15)

In a similar work, these authors compared the performance of Ru- and Rh-based DFM systems synthesized via incipient wetness impregnation on γ -Al₂O₃ using Ru(NO)(NO₃)₃ and Rh(NO₃)₃ as precursors. ¹⁴ The samples were reduced in 4% H₂/N₂ at 320 °C for 2 h, after which a 10% CO₂/N₂ mixture was fed at 320 °C for the CO₂ capture stage. The subsequent methanation step was carried out in a flow of 4% H₂/N₂ for 2 h. On the basis of the results shown in Table 7, it was concluded that the Rh-based DFMs were more active than those containing Ru, obtaining 0.40 g-mol CH₄/kg DFM with only 0.1% Rh loading (0.1% Rh, 10% CaO/γ -Al₂O₃ sample), which is 80% of that obtained with the 5% Ru, 10% $CaO/\gamma - Al_2O_3$ material with a much higher metal loading. Even when Rh is an excellent candidate for applications that require higher resistance to oxidizing conditions, it seems like Ru is still preferred for the development of DFMs based on its activity, stability, and relative low price when compared to Rh (Ru = \$280/troy oz. vs Rh = \$8,600/troy oz. on July 16, $2020)^{78}$

Further work investigated the effect of the different sorbent species on the Ru-based DFM (K_2CO_3 , Na_2CO_3 , and CaO). ¹⁴ To do so, 5% Ru, 10% K_2CO_3/γ -Al₂O₃ and 5% Ru, 10% Na_2CO_3/γ -Al₂O₃ were studied alongside the already reported 5% Ru, 10% CaO/γ -Al₂O₃ DFM. It was observed that both 5% Ru, 10% K_2CO_3/γ -Al₂O₃ and 5% Ru, 10% Na_2CO_3/γ -Al₂O₃ outperformed the 5% Ru, 10% CaO/γ -Al₂O₃ DFM with methanation capacities of 0.91 and 1.05 g-mol CH_4/kg DFM, respectively. Interestingly, these results proved that the higher is the adsorptive capacity of the sorbent species, the more effective the DFM is, as it was shown that the performance was in the order Na_2CO_3 >

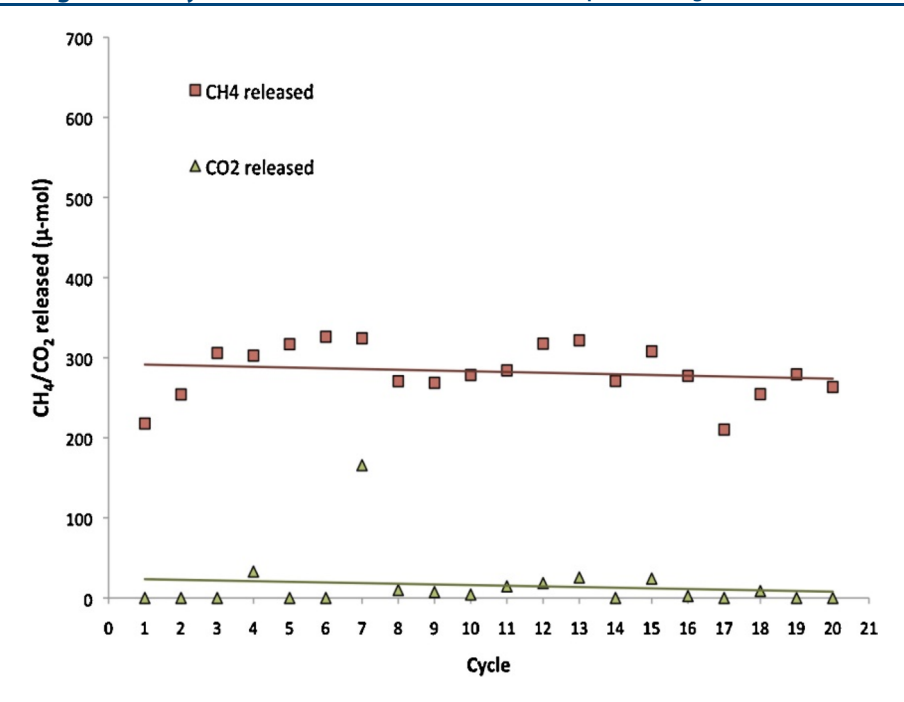


Figure 8. CO₂ and CH₄ released during the 20-cycle test performed under accelerated aging conditions. Reprinted with permission from ref 74. Copyright 2015 Elsevier.

Table 7. Methane Turnover (mol CH₄ Produced/mol of Rh or Ru Present in Sample) and Methanation Capacity Reported over Rh- and Ru-Based DFMs. Reprinted with Permission from ref 14. Copyright 2016 Elsevier

sample	CH ₄ /Rh or Ru	g-mol CH ₄ /kg DFM
10% Rh/ γ -Al ₂ O ₃	0.3	0.30
10% Rh, 10% CaO/γ - Al_2O_3	0.9	0.90
5% Rh, 10% CaO/γ -Al ₂ O ₃	1.3	0.70
1% Rh, 10% CaO/γ -Al ₂ O ₃	7.0	0.70
0.1% Rh, 10% CaO/γ - Al_2O_3	42.0	0.40
5% Ru, 10% CaO/γ -Al ₂ O ₃	1.0	0.50

 $K_2CO_2 > CaO$. This shows that selecting a sorbent with high CO₂ adsorption potential can go a long way to improve the effectiveness of a dual-function material. In the same year, Zheng et al. performed a parametric study on the capture and conversion of CO₂ from a flue gas stream with the same 5% Ru, 10% CaO/ γ -Al₂O₃ DFM. Here, they examined the effect of the synthesis method, shape, and properties of the alumina support, and the conditions for the CO2 adsorption and methanation stages. When comparing the use of chloride precursors (RuCl₃ and CaCl₂) with conventional nitrate salts, they observed a more uniform penetration into the Al₂O₃ particulates when using chloride-based compounds. With regards to the alumina support, the cylindrical pellet-form provided the best methanation performance when compared to the spherical beads and powder forms. CO₂ adsorption and conversion experiments revealed that the reaction temperature affected the kinetics and thermodynamics of the process achieving an optimum at 320 °C. It was also observed that the presence of water and oxygen reduced the adsorption and conversion capacity of the DFM due to the oxidation of the active Ru species. Although high flow rates of hydrogen led to an improved reduction of ruthenium oxide to the active metallic state, the low residence times limited the methanation activity; hence, it was preferred to operate at

moderate feed flow rates. Later on, Wang et al. reported cyclic aging studies with the 5% Ru, 10% Na₂CO₃/γ-Al₂O₃ DFM pellet system for the capture and hydrogenation of CO₂. A 10-cycle aging test was carried out using 7.5% CO₂/N₂ (O₂-free conditions) for CO₂ adsorption and 5% H_2/N_2 for methanation, while a 12-cycle test was run under simulated flue gas conditions (containing O_2), all experiments being performed at 320 °C. As expected, the presence of oxygen led to the formation of Ru oxide (RuOx), which caused a loss in the catalytic activity. After the 10th cycle, the catalyst was regenerated by exposing it to an excess of hydrogen resulting in a recovery of both CO2 adsorption and methanation. Parametric studies performed by the same researchers with a 5% Ru, 6.1% Na₂O/γ-Al₂O₃ DFM system showed the effects that the space velocity (flow rate of feed gas), oxygen exposure time during the capture phase, and the temperature of reaction have on the catalytic performance.⁷⁶ As shown in Figure 9A, the gas space velocity had a negligible effect on the amount of CO2 adsorbed and methane formed, only affecting the rate of the process. It was also observed that both the CO₂ adsorption and methanation steps were slightly hindered when increasing the temperature, which was expected based on the thermodynamics of the processes (Figure 9B). From Figure 9C, they concluded that an increased exposure time to the O2-containing flue gas led to an initial improvement of the CO2 adsorption, but this peaked after 20 min. This also led to an increase in the methanation as the concentration of CO2 increased. Although increased exposure times led to increased oxidation of Ru, a 15% H₂/N₂ gas feed was enough to reduce the catalyst back to its metallic state and initiate the methanation process; hence, no significant loss of activity was observed.

Bermejo-López et al. investigated the mechanism of the CO₂ capture and methanation over Ru-CaO/Al₂O₃ and Ru-Na₂CO₃/Al₂O₃ DFMs.⁷⁷ They noticed that increasing the CaO adsorbent loading led to a reduced Ru dispersion, as confirmed via H₂ chemisorption and microscopy analysis.

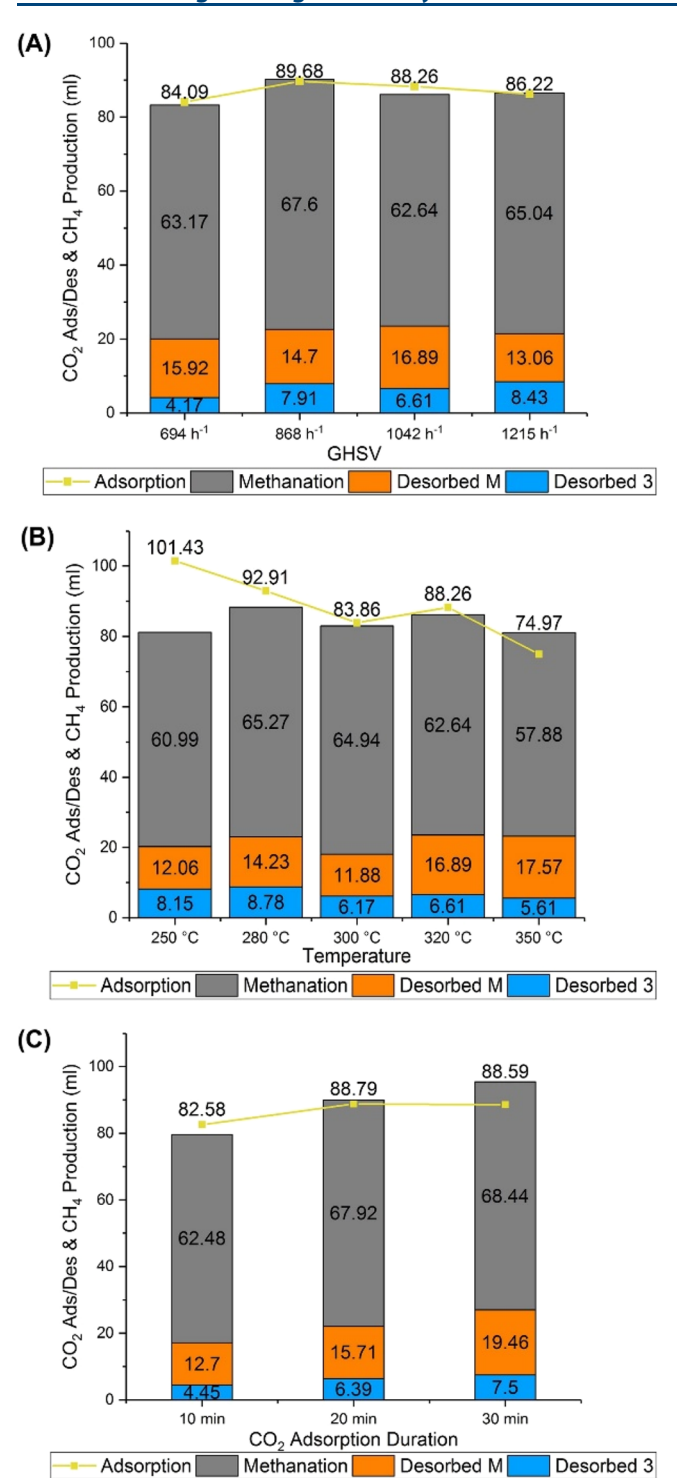


Figure 9. Parametric studies with a 5% Ru, 6.1% $Na_2O/\gamma - Al_2O_3$ DFM system under simulated flue gas conditions: (A) effect of space velocity at 320 °C; (B) temperature effect at 1042 h⁻¹; and (C) O_2 exposure times at 320 °C and 868 h⁻¹. Nomenclature: Desorbed M = CO_2 desorbed during methanation; Desorbed 3 = CO_2 desorbed during N_2 purge. Reprinted with permission from ref 76. Copyright 2018 Elsevier.

Conversely, increased Na₂CO₃ loading had a promotional effect on the dispersion of Ru. As expected, increasing the adsorbent loading increased the catalyst basicity due to the formation of stable carbonate species, an effect that was more pronounced on CaO than on Na₂CO₃ DFM, with TPR

analysis showing a higher reduction temperature to activate the CaO-based DFM. They concluded that the CO₂ adsorption was accompanied by a release of water and the formation of the corresponding hydroxide (NaOH or $Ca(OH)_2$) and that the adsorption primarily happened on the basic oxide (CaO or Na2O) surface and only proceeded on the hydroxide surface once the oxides were fully occupied. The hydrogenation step led to the release of CH₄, H₂O₄ and small quantities of CO, indicating a high selectivity of these DFMs to methane. In-situ DRIFTS studies performed by Proano et al. over a Ru-Na2O/Al2O3 DFM revealed that CO₂ is adsorbed over the sorbent surface forming bidentate carbonates. 80 While CO₂ is adsorbed on Ru active sites, alumina OH groups, and bidentate carbonates on the Ru-Na₂O/Al₂O₃ DFM, this is only adsorbed on Ru active sites and alumina OH groups on a traditional Ru/Al₂O₃ catalyst, which explains the reason for the enhancement in the methanation activity with the DFM. In both cases, during the hydrogenation step (methanation), all CO2 adsorbed behave similarly in that they spill over onto the catalytic Ru sites, where they are hydrogenated forming methane with formates as reaction intermediates.

Although most of the earlier reports are focused on metal oxide- and carbonate-based DFMs, Cimino et al. studied the effect of alkali promoters (Li, Na, K) on the performance of Ru/Al₂O₃.81 These materials were synthesized via sequential impregnation of the ruthenium and alkali precursors, and nitrate and carbonate alkali salts were used to evaluate the effect of the promoter precursor. The Li-Ru catalyst prepared using LiCO3 displayed the highest methanation activity, followed by the Na-promoted Ru catalyst prepared with the sodium nitrate precursor. Both the Na-Ru/AlO₃ and K-Ru/Al₂O₃ DFMs synthesized with carbonate precursors showed poor catalytic activity toward methane production, which was the result of incomplete decomposition of the carbonates at the reduction conditions (400 °C) and the masking effect of the amorphous species on the Ru active sites. In general, the alkali-doped catalysts were 4-5 times more active than the base catalysts for the CO₂ capture process, showing a periodic trend of Li > Na ≥ K. The best DFM, Li-Ru/Al₂O₃, was used to conduct cyclic CO₂ capture and methanation experiments and showed to be highly stable with repeatable results at 230 °C, a temperature much lower than those reported for other Ru-based DFMs.

Indeed, Ru-based DFMs have proved to be highly active in the CO_2 methanation reaction. Remarkably, the energetics of this reaction favors the CO_2 desorption process, allowing for both the CO_2 capture and conversion to be performed isothermally. In addition, Ru-based DFMs exhibit good stability in oxidizing feed conditions due to the facile reduction of RuO_x species. Even when Rh-based DFMs are more active than their Ru counterparts, their high cost limits their use. Further studies are necessary to probe the utilization of Ru-based DFMs in other CO_2 conversion reactions, such as reforming, synthesis of oxygenates, and production of higher hydrocarbons.

4.3. Other Novel DFMs. Bobadilla et al. investigated the use of abundant base metals for the capture and conversion of CO₂ to syngas. They made use of a hydrotalcite-supported FeCrCu-K catalyst synthesized via sequential impregnation. First, the hydrotalcite support was calcined at 600 °C to obtain the homogeneous mixed oxides of MgO and Al₂O₃, after which the incipient wetness method was

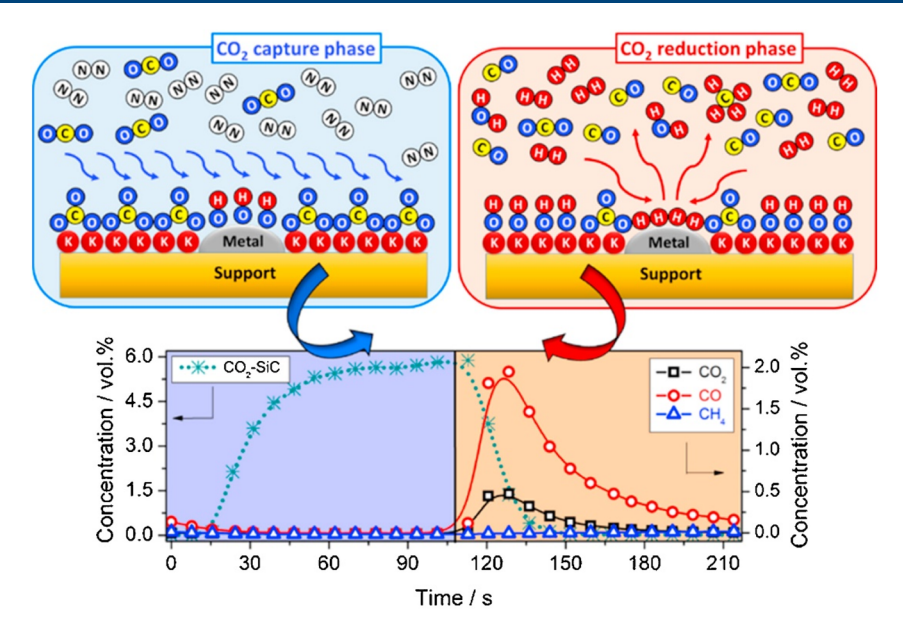


Figure 10. Plausible mechanism for the CO₂ capture and conversion to syngas and representative concentration profiles. For comparison purposes, the CO₂ concentration profile measured using an inert SiC material is also shown. Reprinted with permission from ref 82. Copyright 2016 Elsevier.

used to deposit the metals (Fe, Cr, and Cu) using nitrate precursors. After drying and calcining the sample at 500 $^{\circ}$ C, a K_2 CO $_3$ solution was impregnated over the sample, and this was dried and calcined again at the same temperature. The catalyst was subjected to CO_2 capture using 5.8% CO_2/N_2 and to the hydrogenation step using pure H_2 between 450 and 550 $^{\circ}$ C. The concentration profiles of CO_2 and CO during the capture and reduction stages are shown in Figure 10. As can be seen, CO_2 is effectively adsorbed over the alkali metal (K) forming surface carbonates, and after switching to H_2 , most of the captured CO_2 reacts with H_2 over the catalytic sites (Fe, Cr, and Cu) releasing CO and some unconverted CO_2 .

For more realistic studies, they also explored the use of other CO₂ streams containing water, oxygen, and a mixture of water and oxygen (realistic conditions). In all cases, the capture capacity remained close to 100%, only decreasing slightly at higher CO₂ concentrations (Figure 11). The CO₂ conversion also decreased by 30–25%, which was attributed to the oxidation of the active species by oxygen/water, but the CO selectivity was superior to 90% in all cases (Figure 11). Remarkably, the catalyst showed to be stable after 750 capture/reduction cycles (45 h) at 550 °C in both ideal and realistic feed conditions. The exceptional high stability and CO selectivity here obtained with abundant metals could contribute to the industrial implementation of dual-function materials for CO₂ capture and valorization.

Another example was provided by Hyakutake et al., who studied the effect of promoting a $\text{Cu/Al}_2\text{O}_3$ catalyst with K and Ba for its use in CO_2 capture and conversion with the aim of understanding the fundamental chemical processes and active sites involved on these. They utilized diffuse reflectance infrared fourier transform spectroscopy (DRIFTS), X-ray absorption fine structure (XAFS), and X-ray diffraction (XRD) to gain insights about the structure of the catalyst, surface species, and electronic structure during the capture and reduction processes. They made use of three different samples, $\text{Cu/Al}_2\text{O}_3$, K-promoted ($\text{Cu-K/Al}_2\text{O}_3$),

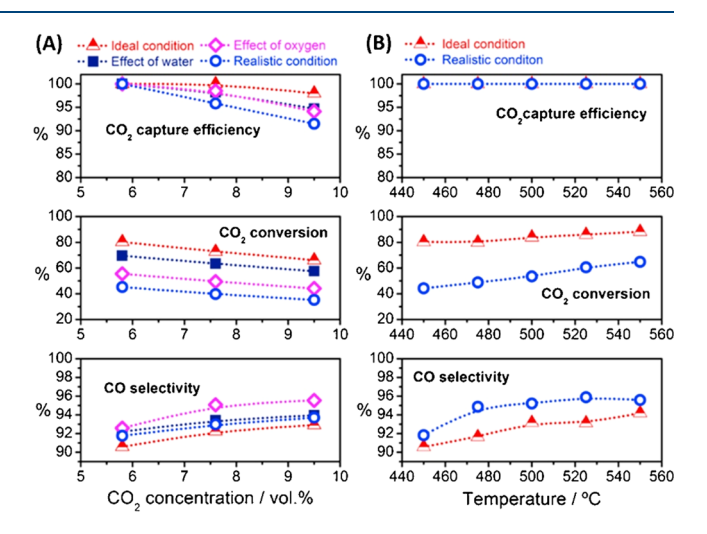


Figure 11. CO_2 conversion and CO selectivity for both ideal and realistic conditions as a function of (A) CO_2 concentration at 450 $^{\circ}C$ and (B) reaction temperature. Reprinted with permission from ref 82. Copyright 2016 Elsevier.

and Ba-promoted ($Cu-Ba/Al_2O_3$) for the CO_2 capture and reduction processes at 350 °C using a 4.4% CO_2/He stream and pure H_2 , respectively. The $Cu-K/Al_2O_3$ DFM showed the best behavior, capturing CO_2 efficiently as formate species and subsequently converting them into CO upon exposure to hydrogen (Figure 12). The bare Cu/Al_2O_3 catalyst, on the other hand, displayed a different mechanism, with predominant formation of CO during the capture step, which was attributed to the surface oxidation of Cu. A mixed activity was observed when using the $Cu-Ba/Al_2O_3$ sample, observing a notable formation of CO during both the capture and reduction steps (Figure 12). Although the Ba-promoted ($Cu-Ba/Al_2O_3$) catalyst could capture CO_2 to some extent, this catalyst was inefficient in fully capturing CO_2 with a large amount of uncaptured CO_2 observed in the effluent stream.

XAFS studies showed that Cu remained free from oxidation on the K-promoted catalyst and XRD spectra

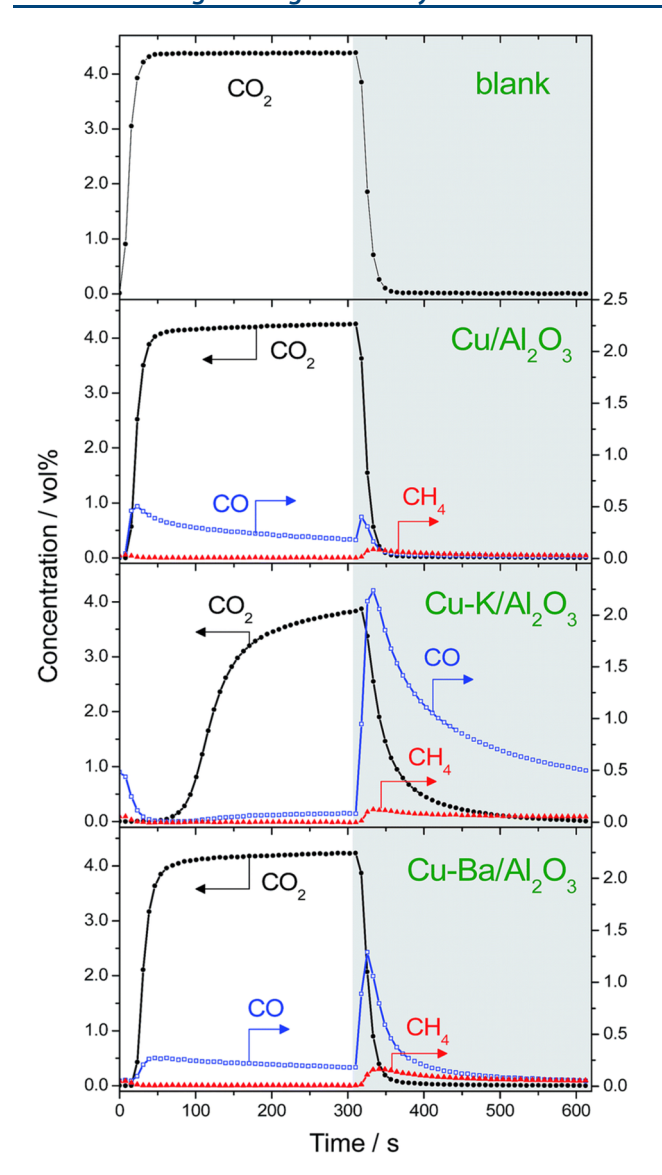


Figure 12. CO₂ and reaction products (CO and CH₄) concentration profiles during CO₂ capture and conversion. Republished with permission from ref 83. Copyright 2016 Royal Society of Chemistry; permission conveyed through Copyright Clearance Center, Inc.

showed no diffraction peaks corresponding to metallic Cu, which confirmed the high dispersion and small particle size. DRIFTS confirmed the presence of formate species, which is an intermediate commonly reported for CO and methanol formation. These studies also showed that formate species were in contact with K, suggesting that K provided some coverage over Cu that ultimately inhibited its oxidation. These characteristics explained the reason for which the K-promoted Cu catalyst was more active than the unpromoted Cu and Ba-promoted Cu catalysts. The mechanistic insights provided in this work could pave a way for designing more effective dual-function materials for CO₂ conversion, especially using abundant earth metals, such as Cu.

More recently, Al-Mamoori et al.⁸⁴ investigated the use of potassium- and sodium-based calcium oxide double salts (K—Ca and Na—Ca) adsorbents physically mixed with a H-ZSM-5-supported Cr catalyst for the oxidative dehydrogenation of ethane (ODHE) using CO₂ as a mild oxidant (eq 16).⁸⁵ This

reaction is especially attractive as ethylene is one of the most important building blocks in the chemical industry.

$$C_2H_6 + CO_2 \leftrightharpoons C_2H_4 + CO + H_2O;$$

 $\Delta H_r^{\circ} = +179.0 \text{ kJ mol}^{-1}$ (16)

The authors observed a higher CO₂ uptake when using double salts when compared to a base study performed with a mixture of CaO and the catalyst. While the (K-Ca)/Cr/H-ZSM-5 material displayed a CO₂ sorption capacity of 5.2 mmol/g, the sorption capacities of (Na-Ca)/Cr/H-ZSM-5 and CaO/Cr/H-ZSM-5 were 3.2 mmol/g and 0.8 mmol/g, respectively. This improved adsorption on the double salts was attributed to the formation of double carbonates (K₂Ca(CO₃)₂ and Na₂Ca(CO₃)₂). In addition, they studied the effect of the Cr content and the C2H6 feed composition on the effectiveness of the DFM. It was observed that as the Cr content was increased, the CO₂ and C₂H₆ conversion increased up to a maximum with 10 wt % Cr, and subsequently decreased as the Cr content was increased to 15 wt %. This decrease in activity when using 15 wt % Cr loading was attributed to a poor dispersion and the formation of a α -Cr₂O₃ phase, which limited the selectivity toward C₂H₆. Further, it was shown that although the C₂H₄ selectivity was reduced from 96.7 to 45.7% upon decreasing the C₂H₆ feed concentration from 5 to 1 vol %, the C₂H₆ conversion increased from 18.3 to 45.7%. This effect was correlated to the prevalence of the RWGS reaction at lower C₂H₆ concentrations, which leads to the consumption of H₂ produced, promoting the conversion of C₂H₆ and invariably leading to increased C2H4 yield. Although cyclic studies revealed sintering and coke formation over the material, this work opens more avenues to harness CO2 to produce light olefins, which are highly industrially relevant.

These recent approaches using earth abundant metals such as Cu and Cr are inherently economically viable and can immensely benefit the development of DFM technology. Further investigations should focus on the improvement of the activity and stability of these base metal DFM systems. It is worth highlighting the number of reactions that can be carried out with this type of materials, such as the important ODHE reaction to produce ethylene using Cr-based DFMs. However, this particular reaction is still under investigation, as it competes with the dry ethane reforming reaction to produce CO, which was predominant when using Ni-based DFMs under similar reaction conditions. The optimization of the process together with the elucidation of the active sites involved in the different mechanisms could go a long way in steering future research efforts.

5. CONCLUSIONS, CHALLENGES, AND OPPORTUNITIES

In this review, we summarized the use of dual-function materials for CO_2 capture and conversion to value-added products. To properly discuss the DFM structures, we first took a close look at the different adsorbents used as the capture component on DFMs. Oxides and carbonates are excellent adsorbents for CO_2 capture since they are inexpensive, abundant, and have high reactivity toward CO_2 . However, sometimes these adsorbents suffer from irreversible carbonation due to sintering and loss of reactivity after multiple sorption/desorption cycles. These challenges have been addressed by dispersing the adsorbents on a

support, by modification of the synthesis protocols, and by introduction of dopant species. These techniques were reported to help increase the sorption capacity of these oxides and carbonates and enabled the adsorbents to retain their stability after several cycles.

To provide a good perspective to the reader, we categorized the commonly used DFMs by the catalytic metal component. Ni-based DFMs have displayed good CO2 sorption capacities and adequate reactivities and have been reported for a wide range of applications, including production of methane and synthesis gas, and dry reforming of methane and ethane. Although Ni is an affordable and abundant metal and displays good activity for these reactions, it possesses some drawbacks that have limited its applicability. First, Ni-based DFMs require high reduction temperatures (typically >600 °C), which implies a high energy consumption. Further, Ni-based DFMs easily deactivate under simulated flue gas conditions (containing oxygen and water) due to the formation of NiO species that are not easily reduced under reaction conditions. The introduction of noble metals (Pd and Pt) has been reported to improve the reducibility of Ni; however, there exists a trade off in the reduction of the methanation rates, and the challenges associated with the cost of these noble metals make this alternative less profitable.

Ru-based DFM structures, on the other hand, are effective at lower temperature reactions (~320 °C). Also, Ru-based systems can operate isothermally for both capture and conversion, making the process highly energy efficient. The energetics of Ru-based DFMs is favorable owing to the fact that much of the implementation has been limited to the methanation reaction, which is exothermic and allows for heat integration with the CO₂ desorption process. In addition, Ru-based DFMs exhibit good stability in oxidizing feed conditions due to the facile reduction of RuOx species. These advantages have enabled Ru-based DFMs to gain more traction compared to their Ni counterparts despite their higher cost. However, the use of Ru-based DFMs have mostly been limited to methanation reactions, and more studies would be needed to investigate their activity toward CO synthesis or reforming-based reactions, as in the case of Ni-based DFMs. A combined approach using both Ni and Ru to create bimetallic DFMs was reported to enhance the activity for methane production, and similar systems could be explored for other reactions in which Ni has proven to be active. In addition, owing to the fact that chemisorption is the main sorption process in DFMs and poisons could easily bond to the sorbent sites, it would be beneficial to study the effectiveness of these DFMs under real exhaust gas conditions, in which impurities such as NO_x and SO_x are present. These findings would bolster the industrial applicability of these materials.

Recent reports have shown the use of Cu-based systems for the capture and conversion of CO₂ to produce syngas. Owing to the abundant nature of Cu and the dopant species explored, as well as the high activity of these materials even under simulated flue gas conditions, it would be interesting to further develop Cu-based DFMs for CO₂ capture and conversion

As the development of DFMs is in its infancy, most of the publications have focused on the incorporation of sorbents and catalytic species by impregnation techniques; however, we believe that the future of the field is in the design of well-

controlled nanoarchitectures with catalytic and sorbent components in close proximity for improved synergy. An almost neglected avenue in the area of DFMs is their use in the production of higher energy density products, such as alcohols or higher hydrocarbons. As Cu-based catalysts have been typically employed for methanol production, we believe that the utilization of Cu-based DFMs could be a starting point in establishing these efforts.

AUTHOR INFORMATION

Corresponding Author

Ana C. Alba-Rubio — Department of Chemical Engineering, The University of Toledo, Toledo, Ohio 43606, United States; orcid.org/0000-0002-1831-8338; Email: ana.albarubio@utoledo.edu

Authors

Ibeh S. Omodolor — Department of Chemical Engineering, The University of Toledo, Toledo, Ohio 43606, United States Hope O. Otor — Department of Chemical Engineering, The University of Toledo, Toledo, Ohio 43606, United States Joseph A. Andonegui — Department of Chemical Engineering, The University of Toledo, Toledo, Ohio 43606, United States Bryan J. Allen — Department of Chemical Engineering, The University of Toledo, Toledo, Ohio 43606, United States

Complete contact information is available at: https://pubs.acs.org/10.1021/acs.iecr.0c02218

Author Contributions

[†]I.S.O. and H.O.O.: Equal contribution.

Notes

The authors declare no competing financial interest.

Biographies



Ibeh Omodolor received his bachelor's degree in chemical engineering from the University of Lagos, Nigeria, and his M.S. degree from the Institute of Petroleum Studies Port Harcourt. Currently, he is a 4th year Ph.D. candidate working under the supervision of Dr. Alba-Rubio in the Department of Chemical Engineering at the University of Toledo. For the past three years, he developed soluble and reusable polymer catalysts for the synthesis of hydroxymethylfurfural from glucose, and right now, he is focused on the development of dual-function materials for CO_2 capture and conversion into value-added products.



Hope Otor obtained his bachelor's degree in chemical engineering from the Federal University of Technology, Minna, Nigeria. He recently completed his master's program in chemical engineering at the University of Toledo under the supervision of Prof. Ana C. Alba-Rubio with a thesis focused on catalyst development and control of catalyst deactivation for ${\rm CO_2}$ conversion. Hope is currently a Ph.D. student in the Department of Chemical and Biomolecular Engineering at the University of Notre Dame. His primary research interests are in catalytic systems and sustainable energy applications.



Joseph Andonegui received his bachelor's degree in chemical engineering from the University of Toledo in 2020. During his undergraduate studies, he conducted research at the Alba-Rubio's research group with focus on synthesis and characterization of catalysts for ${\rm CO}_2$ conversion. He is currently employed as a COVID-19 vaccine formulation technician and operator at AstraZeneca pharmaceuticals.



Bryan J. Allen is an undergraduate student at the University of Toledo. He will graduate with a bachelor's in chemical engineering

with a chemistry minor in December 2020. His research interests lie in environmental sustainability efforts, with previous research focusing on the development of electrocatalysts for use in anion exchange membrane fuel cells as well as catalysts for ${\rm CO}_2$ conversion and plasma synthesis of ammonia. Upon graduation, he plans to continue doing research outside of academia.



Dr. Ana C. Alba-Rubio is an Assistant Professor in the Department of Chemical Engineering at the University of Toledo. She received a bachelor's degree in chemical engineering from the University of Málaga, Spain, in 2007. She then moved to the Institute of Catalysis and Petrochemistry (CSIC) in Madrid, Spain, to pursue her doctoral studies. After completing her postdoctoral stage at the University of Wisconsin-Madison, she joined the University of Toledo as a faculty in 2015. Her current research interests involve the rational design and synthesis of nanomaterials for catalysis and sensing applications, with a particular interest in producing fuels and materials sustainably and improving the human condition. She has authored 24 publications in peer-reviewed journals with more than 1400 citations (h = 18), one book chapter, 5 patent applications, and 60 contributions to national and international conferences. She has received numerous awards, including the National Science Foundation CAREER Award (2019), the 2018 UToledo President's Award for Outstanding Contributions in Scholarship and Creative Activity, and the 2019 UToledo College of Engineering Excellence in Supervision of Undergraduate Research Award.

ACKNOWLEDGMENTS

This invited contribution is part of the I&EC Research special issue for the 2020 Class of Influential Researchers. This material is based upon work supported by the National Science Foundation under Grant No. 1847391. Authors are also thankful to G. Alba and J. Andonegui for the design of the graphical abstract.

REFERENCES

- (1) Jiang, X.; Wang, X.; Nie, X.; Koizumi, N.; Guo, X.; Song, C. CO2 hydrogenation to methanol on Pd-Cu bimetallic catalysts: H2/CO2 ratio dependence and surface species. *Catal. Today* **2018**, *316*, 62–70.
- (2) Al-Mamoori, A.; Rownaghi, A. A.; Rezaei, F. Combined Capture and Utilization of CO2 for Syngas Production over Dual-Function Materials. *ACS Sustainable Chem. Eng.* **2018**, 6 (10), 13551–13561.
- (3) Jiang, Z.; Xiao, T.; Kuznetsov, V. L.; Edwards, P. P. Turning carbon dioxide into fuel. *Philos. Trans. R. Soc., A* **2010**, 368 (1923), 3343–64.
- (4) Song, C. Global challenges and strategies for control, conversion and utilization of CO2 for sustainable development

- involving energy, catalysis, adsorption and chemical processing. *Catal. Today* **2006**, *115* (1–4), 2–32.
- (5) Centi, G.; Perathoner, S. Opportunities and prospects in the chemical recycling of carbon dioxide to fuels. *Catal. Today* **2009**, *148* (3–4), 191–205.
- (6) Aresta, M.; Dibenedetto, A. The contribution of the utilization option to reducing the CO2 atmospheric loading: research needed to overcome existing barriers for a full exploitation of the potential of the CO2 use. *Catal. Today* **2004**, *98* (4), 455–462.
- (7) Markewitz, P.; Kuckshinrichs, W.; Leitner, W.; Linssen, J.; Zapp, P.; Bongartz, R.; Schreiber, A.; Müller, T. E. Worldwide innovations in the development of carbon capture technologies and the utilization of CO2. *Energy Environ. Sci.* **2012**, *5* (6), 7281–7305.
- (8) Yu, K. M.; Curcic, I.; Gabriel, J.; Tsang, S. C. Recent advances in CO2 capture and utilization. *ChemSusChem* **2008**, *1* (11), 893–9.
- (9) Alami, A. H.; Abu Hawili, A.; Tawalbeh, M.; Hasan, R.; Al Mahmoud, L.; Chibib, S.; Mahmood, A.; Aokal, K.; Rattanapanya, P. Materials and logistics for carbon dioxide capture, storage and utilization. *Sci. Total Environ.* **2020**, *717*, 137221.
- (10) Cuéllar-Franca, R. M.; Azapagic, A. Carbon capture, storage and utilisation technologies: A critical analysis and comparison of their life cycle environmental impacts. *J. CO2 Util.* **2015**, *9*, 82–102.
- (11) Mondal, M. K.; Balsora, H. K.; Varshney, P. Progress and trends in CO2 capture/separation technologies: A review. *Energy* **2012**, 46 (1), 431–441.
- (12) Al-Mamoori, A.; Krishnamurthy, A.; Rownaghi, A. A.; Rezaei, F. Carbon Capture and Utilization Update. *Energy Technol.* **2017**, *5* (6), 834–849.
- (13) Zhao, C.; Chen, X.; Anthony, E. J.; Jiang, X.; Duan, L.; Wu, Y.; Dong, W.; Zhao, C. Capturing CO2 in flue gas from fossil fuel-fired power plants using dry regenerable alkali metal-based sorbent. *Prog. Energy Combust. Sci.* **2013**, *39* (6), 515–534.
- (14) Duyar, M. S.; Wang, S.; Arellano-Treviño, M. A.; Farrauto, R. J. CO 2 utilization with a novel dual function material (DFM) for capture and catalytic conversion to synthetic natural gas: An update. *J. CO2 Util.* **2016**, *15*, 65–71.
- (15) Dutcher, B.; Fan, M.; Russell, A. G. Amine-based CO2 capture technology development from the beginning of 2013-a review. ACS Appl. Mater. Interfaces 2015, 7 (4), 2137–48.
- (16) Zhang, W.; Liu, H.; Sun, Y.; Cakstins, J.; Sun, C.; Snape, C. E. Parametric study on the regeneration heat requirement of an amine-based solid adsorbent process for post-combustion carbon capture. *Appl. Energy* **2016**, *168*, 394–405.
- (17) Zhao, G. J. a. M., Membrane Separation Technology in Carbon Capture. In *Recent Advances in Carbon Capture and Storage*; Intech: 2017; pp 59–90.
- (18) Wang, Q.; Luo, J.; Zhong, Z.; Borgna, A. CO2 capture by solid adsorbents and their applications: current status and new trends. *Energy Environ. Sci.* **2011**, *4* (1), 42–55.
- (19) Lee, C. H.; Mun, S.; Lee, K. B. Characteristics of Na–Mg double salt for high-temperature CO2 sorption. *Chem. Eng. J.* **2014**, 258, 367–373.
- (20) Li, L.; King, D. L.; Nie, Z.; Howard, C. Magnesia-Stabilized Calcium Oxide Absorbents with Improved Durability for High Temperature CO2 Capture. *Ind. Eng. Chem. Res.* **2009**, 48 (23), 10604–10613.
- (21) Gruene, P.; Belova, A. G.; Yegulalp, T. M.; Farrauto, R. J.; Castaldi, M. J. Dispersed Calcium Oxide as a Reversible and Efficient CO2–Sorbent at Intermediate Temperatures. *Ind. Eng. Chem. Res.* **2011**, *50* (7), 4042–4049.
- (22) Sun, H.; Wu, C.; Shen, B.; Zhang, X.; Zhang, Y.; Huang, J. Progress in the development and application of CaO-based adsorbents for CO2 capture—a review. *Materials Today Sustainability* **2018**, *1*–2, 1–27.
- (23) Florin, N. H.; Harris, A. T. Reactivity of CaO derived from nano-sized CaCO3 particles through multiple CO2 capture-and-release cycles. *Chem. Eng. Sci.* **2009**, *64* (2), 187–191.
- (24) Li, Y. J.; Zhao, C. S.; Qu, C. R.; Duan, L. B.; Li, Q. Z.; Liang, C. CO2 Capture Using CaO Modified with Ethanol/Water Solution

- during Cyclic Calcination/Carbonation. Chem. Eng. Technol. 2008, 31 (2), 237-244.
- (25) Granados-Pichardo, A.; Granados-Correa, F.; Sánchez-Mendieta, V.; Hernández-Mendoza, H. New CaO-based adsorbents prepared by solution combustion and high-energy ball-milling processes for CO2 adsorption: Textural and structural influences. *Arabian J. Chem.* **2020**, *13* (1), 171–183.
- (26) Belova, A. A. G.; Yegulalp, T. M.; Yee, C. T. Feasibility study of In Situ CO2 capture on an integrated catalytic CO2 sorbent for hydrogen production from methane. *Energy Procedia* **2009**, *1* (1), 749–755.
- (27) Antzara, A.; Heracleous, E.; Lemonidou, A. A. Improving the stability of synthetic CaO-based CO 2 sorbents by structural promoters. *Appl. Energy* **2015**, *156*, 331–343.
- (28) Guo, H.; Kou, X.; Zhao, Y.; Wang, S.; Sun, Q.; Ma, X. Effect of synergistic interaction between Ce and Mn on the CO2 capture of calcium-based sorbent: Textural properties, electron donation, and oxygen vacancy. *Chem. Eng. J.* **2018**, 334, 237–246.
- (29) Al-Mamoori, A.; Lawson, S.; Rownaghi, A. A.; Rezaei, F. Improving Adsorptive Performance of CaO for High-Temperature CO2 Capture through Fe and Ga Doping. *Energy Fuels* **2019**, 33 (2), 1404–1413.
- (30) Yoshikawa, K.; Sato, H.; Kaneeda, M.; Kondo, J. N. Synthesis and analysis of CO2 adsorbents based on cerium oxide. *J. CO2 Util.* **2014**, *8*, 34–38.
- (31) Liang, Y.; Harrison, D. P.; Gupta, R. P.; Green, D. A.; McMichael, W. J. Carbon Dioxide Capture Using Dry Sodium-Based Sorbents. *Energy Fuels* **2004**, *18*, 569–575.
- (32) Kondakindi, R. R.; McCumber, G.; Aleksic, S.; Whittenberger, W.; Abraham, M. A. Na2CO3-based sorbents coated on metal foil: CO2 capture performance. *Int. J. Greenhouse Gas Control* **2013**, *15*, 65–69.
- (33) Yu, F.; Wu, Y.; Zhang, W.; Cai, T.; Xu, Y.; Chen, X. A novel aerogel sodium-based sorbent for low temperature CO2capture. *Greenhouse Gases: Sci. Technol.* **2016**, *6* (4), 561–573.
- (34) Zhao, C.; Chen, X.; Zhao, C. Effect of crystal structure on CO2 capture characteristics of dry potassium-based sorbents. *Chemosphere* **2009**, 75 (10), 1401–1404.
- (35) Zhao, C.; Chen, X.; Zhao, C. Multiple-Cycles Behavior of K2CO3/Al2O3for CO2Capture in a Fluidized-Bed Reactor. *Energy Fuels* **2010**, 24 (2), 1009–1012.
- (36) Lee, S. C.; Kwon, Y. M.; Jung, S. Y.; Lee, J. B.; Ryu, C. K.; Kim, J. C. Excellent thermal stability of potassium-based sorbent using ZrO2 for post combustion CO2 capture. *Fuel* **2014**, *115*, 97–100
- (37) Wu, Y.; Chen, X.; Zhao, C. Study on the failure mechanism of potassium-based sorbent for CO2 capture and the improving measure. *Int. J. Greenhouse Gas Control* **2011**, *5* (5), 1184–1189.
- (38) Wu, Y.; Chen, X.; Radosz, M.; Fan, M.; Dong, W.; Zhang, Z.; Yang, Z. Inexpensive calcium-modified potassium carbonate sorbent for CO2 capture from flue gas: Improved SO2 resistance, enhanced capacity and stability. *Fuel* **2014**, *125*, 50–56.
- (39) Melo Bravo, P.; Debecker, D. P. Combining CO2 capture and catalytic conversion to methane. *Waste Disposal & Sustainable Energy* **2019**, *1* (1), 53–65.
- (40) Berger, A. H.; Bhown, A. S. Comparing physisorption and chemisorption solid sorbents for use separating CO2 from flue gas using temperature swing adsorption. *Energy Procedia* **2011**, *4*, 562–567.
- (41) Du, G.; Lim, S.; Yang, Y.; Wang, C.; Pfefferle, L.; Haller, G. Methanation of carbon dioxide on Ni-incorporated MCM-41 catalysts: The influence of catalyst pretreatment and study of steady-state reaction. *J. Catal.* **2007**, 249 (2), 370–379.
- (42) Aziz, M. A. A.; Jalil, A. A.; Triwahyono, S.; Mukti, R. R.; Taufiq-Yap, Y. H.; Sazegar, M. R. Highly active Ni-promoted mesostructured silica nanoparticles for CO2 methanation. *Appl. Catal., B* **2014**, *147*, 359–368.
- (43) Mutz, B.; Carvalho, H. W. P.; Mangold, S.; Kleist, W.; Grunwaldt, J.-D. Methanation of CO2: Structural response of a Ni-

- based catalyst under fluctuating reaction conditions unraveled by operando spectroscopy. *J. Catal.* **2015**, *327*, 48–53.
- (44) Liu, H.; Zou, X.; Wang, X.; Lu, X.; Ding, W. Effect of CeO2 addition on Ni/Al2O3 catalysts for methanation of carbon dioxide with hydrogen. *J. Nat. Gas Chem.* **2012**, *21* (6), 703–707.
- (45) Song, H.; Yang, J.; Zhao, J.; Chou, L. Methanation of Carbon Dioxide over a Highly Dispersed Ni/La2O3 Catalyst. *Chin. J. Catal.* **2010**, *31* (1), 21–23.
- (46) Cai, M.; Wen, J.; Chu, W.; Cheng, X.; Li, Z. Methanation of carbon dioxide on Ni/ZrO2-Al2O3 catalysts: Effects of ZrO2 promoter and preparation method of novel ZrO2-Al2O3 carrier. *J. Nat. Gas Chem.* **2011**, 20 (3), 318–324.
- (47) da Silva, D. C. D.; Letichevsky, S.; Borges, L. E. P.; Appel, L. G. The Ni/ZrO2 catalyst and the methanation of CO and CO2. *Int. J. Hydrogen Energy* **2012**, *37* (11), 8923–8928.
- (48) Wolf, A.; Jess, A.; Kern, C. Syngas Production via Reverse Water-Gas Shift Reaction over a Ni-Al2O3 Catalyst: Catalyst Stability, Reaction Kinetics, and Modeling. *Chem. Eng. Technol.* **2016**, 39 (6), 1040–1048.
- (49) Yang, L.; Pastor-Pérez, L.; Gu, S.; Sepúlveda-Escribano, A.; Reina, T. R. Highly efficient Ni/CeO2-Al2O3 catalysts for CO2 upgrading via reverse water-gas shift: Effect of selected transition metal promoters. *Appl. Catal., B* **2018**, 232, 464–471.
- (50) Wang, L.; Zhang, S.; Liu, Y. Reverse water gas shift reaction over Co-precipitated Ni-CeO2 catalysts. *J. Rare Earths* **2008**, *26* (1), 66–70.
- (51) Wang, L.; Liu, H.; Liu, Y.; Chen, Y.; Yang, S. Influence of preparation method on performance of Ni-CeO2 catalysts for reverse water-gas shift reaction. *J. Rare Earths* **2013**, *31* (6), 559–564
- (52) Sun, F.-m.; Yan, C.-f.; Wang, Z.-d.; Guo, C.-q.; Huang, S.-l. Ni/Ce–Zr–O catalyst for high CO2 conversion during reverse water gas shift reaction (RWGS). *Int. J. Hydrogen Energy* **2015**, 40 (46), 15985–15993.
- (53) Abdullah, B.; Abd Ghani, N. A.; Vo, D.-V. N. Recent advances in dry reforming of methane over Ni-based catalysts. *J. Cleaner Prod.* **2017**, *162*, 170–185.
- (54) Li, X.; Li, D.; Tian, H.; Zeng, L.; Zhao, Z.-J.; Gong, J. Dry reforming of methane over Ni/La2O3 nanorod catalysts with stabilized Ni nanoparticles. *Appl. Catal., B* **2017**, *202*, 683–694.
- (55) Guo, J.; Lou, H.; Zhao, H.; Chai, D.; Zheng, X. Dry reforming of methane over nickel catalysts supported on magnesium aluminate spinels. *Appl. Catal., A* **2004**, *273* (1–2), 75–82.
- (56) Kambolis, A.; Matralis, H.; Trovarelli, A.; Papadopoulou, C. Ni/CeO2-ZrO2 catalysts for the dry reforming of methane. *Appl. Catal., A* **2010**, 377 (1–2), 16–26.
- (57) Ay, H.; Üner, D. Dry reforming of methane over CeO2 supported Ni, Co and Ni-Co catalysts. *Appl. Catal., B* **2015**, *179*, 128–138.
- (58) Olafsen, A.; Daniel, C.; Schuurman, Y.; Råberg, L. B.; Olsbye, U.; Mirodatos, C. Light alkanes CO2 reforming to synthesis gas over Ni based catalysts. *Catal. Today* **2006**, *115* (1–4), 179–185.
- (59) Olafsen, A.; Slagtern, A.; Dahl, I.; Olsbye, U.; Schuurman, Y.; Mirodatos, C. Mechanistic features for propane reforming by carbon dioxide over a Ni/Mg(Al)O hydrotalcite-derived catalyst. *J. Catal.* **2005**, 229 (1), 163–175.
- (60) Tian, S.; Yan, F.; Zhang, Z.; Jiang, J. Calcium-looping reforming of methane realizes in situ CO2 utilization with improved energy efficiency. *Sci. Adv.* **2019**, *5* (4), eaav5077.
- (61) Kim, S. M.; Abdala, P. M.; Broda, M.; Hosseini, D.; Copéret, C.; Müller, C. Integrated CO2 Capture and Conversion as an Efficient Process for Fuels from Greenhouse Gases. *ACS Catal.* **2018**, 8 (4), 2815–2823.
- (62) Sun, H.; Wang, J.; Zhao, J.; Shen, B.; Shi, J.; Huang, J.; Wu, C. Dual functional catalytic materials of Ni over Ce-modified CaO sorbents for integrated CO2 capture and conversion. *Appl. Catal., B* **2019**, 244, 63–75.
- (63) Bermejo-López, A.; Pereda-Ayo, B.; González-Marcos, J. A.; González-Velasco, J. R. Ni loading effects on dual function materials

- for capture and in-situ conversion of CO2 to CH4 using CaO or Na2CO3. *J. CO2 Util.* **2019**, 34, 576–587.
- (64) Arellano-Treviño, M. A.; He, Z.; Libby, M. C.; Farrauto, R. J. Catalysts and adsorbents for CO2 capture and conversion with dual function materials: Limitations of Ni-containing DFMs for flue gas applications. *J. CO2 Util.* **2019**, *31*, 143–151.
- (65) Yan, B.; Yang, X.; Yao, S.; Wan, J.; Myint, M.; Gomez, E.; Xie, Z.; Kattel, S.; Xu, W.; Chen, J. G. Dry Reforming of Ethane and Butane with CO2 over PtNi/CeO2 Bimetallic Catalysts. *ACS Catal.* **2016**, 6 (11), 7283–7292.
- (66) Arellano-Treviño, M. A.; Kanani, N.; Jeong-Potter, C. W.; Farrauto, R. J. Bimetallic catalysts for CO2 capture and hydrogenation at simulated flue gas conditions. *Chem. Eng. J.* **2019**, 375, 121953.
- (67) Wu, C.; Williams, P. T. A novel Ni–Mg–Al–CaO catalyst with the dual functions of catalysis and CO2 sorption for H2 production from the pyrolysis–gasification of polypropylene. *Fuel* **2010**, 89 (7), 1435–1441.
- (68) Di Felice, L.; Courson, C.; Foscolo, P. U.; Kiennemann, A. Iron and nickel doped alkaline-earth catalysts for biomass gasification with simultaneous tar reformation and CO2 capture. *Int. J. Hydrogen Energy* **2011**, *36* (9), 5296–5310.
- (69) Janke, C.; Duyar, M. S.; Hoskins, M.; Farrauto, R. Catalytic and adsorption studies for the hydrogenation of CO2 to methane. *Appl. Catal.*, B **2014**, *152–153*, 184–191.
- (70) Garbarino, G.; Bellotti, D.; Riani, P.; Magistri, L.; Busca, G. Methanation of carbon dioxide on Ru/Al 2 O 3 and Ni/Al 2 O 3 catalysts at atmospheric pressure: Catalysts activation, behaviour and stability. *Int. J. Hydrogen Energy* **2015**, *40* (30), 9171–9182.
- (71) Duyar, M. S.; Ramachandran, A.; Wang, C.; Farrauto, R. J. Kinetics of CO2 methanation over Ru/ γ -Al2O3 and implications for renewable energy storage applications. *J. CO2 Util.* **2015**, *12*, 27–33.
- (72) Kim, A.; Sanchez, C.; Haye, B.; Boissière, C.; Sassoye, C.; Debecker, D. P. Mesoporous TiO2 Support Materials for Ru-Based CO2Methanation Catalysts. *ACS Appl. Nano Mater.* **2019**, 2 (5), 3220–3230.
- (73) Wang, S.; Schrunk, E. T.; Mahajan, H.; Farrauto, a. R. J. The Role of Ruthenium in CO2 Capture and Catalytic Conversion to Fuel by Dual Function Materials (DFM). *Catalysts* **2017**, *7* (3), 88.
- (74) Duyar, M. S.; Treviño, M. A. A.; Farrauto, R. J. Dual function materials for CO 2 capture and conversion using renewable H 2. *Appl. Catal., B* **2015**, *168*–*169*, 370–376.
- (75) Wang, S.; Schrunk, E. T.; Mahajan, H.; Farrauto, a. R. J. The Role of Ruthenium in CO2 Capture and Catalytic Conversion to Fuel by Dual Function Materials (DFM). *Catalysts* **2017**, *7* (3), 88.
- (76) Wang, S.; Farrauto, R. J.; Karp, S.; Jeon, J. H.; Schrunk, E. T. Parametric, cyclic aging and characterization studies for CO2 capture from flue gas and catalytic conversion to synthetic natural gas using a dual functional material (DFM). *J. CO2 Util.* **2018**, 27, 390–397.
- (77) Bermejo-López, A.; Pereda-Ayo, B.; González-Marcos, J. A.; González-Velasco, J. R. Mechanism of the CO2 storage and in situ hydrogenation to CH4. Temperature and adsorbent loading effects over Ru-CaO/Al2O3 and Ru-Na2CO3/Al2O3 catalysts. *Appl. Catal., B* **2019**, 256, 117845.
- (78) Engelhard Industrial Bullion (EIB) Prices [USD per Troy Ounce].https://apps.catalysts.basf.com/apps/eibprices/mp/ (accessed on May 1, 2020).
- (79) Zheng, Q.; Farrauto, R.; Chau Nguyen, A. Adsorption and Methanation of Flue Gas CO2 with Dual Functional Catalytic Materials: A Parametric Study. *Ind. Eng. Chem. Res.* **2016**, *55* (24), 6768–6776.
- (80) Proaño, L.; Tello, E.; Arellano-Trevino, M. A.; Wang, S.; Farrauto, R. J.; Cobo, M. In-situ DRIFTS study of two-step CO2 capture and catalytic methanation over Ru, "Na2O"/Al2O3 Dual Functional Material. *Appl. Surf. Sci.* **2019**, 479, 25–30.
- (81) Cimino, S.; Boccia, F.; Lisi, L. Effect of alkali promoters (Li, Na, K) on the performance of Ru/Al2O3 catalysts for CO2 capture and hydrogenation to methane. *J. CO2 Util.* **2020**, *37*, 195–203.

- (82) Bobadilla, L. F.; Riesco-García, J. M.; Penelás-Pérez, G.; Urakawa, A. Enabling continuous capture and catalytic conversion of flue gas CO 2 to syngas in one process. *J. CO2 Util.* **2016**, *14*, 106–111.
- (83) Hyakutake, T.; van Beek, W.; Urakawa, A. Unravelling the nature, evolution and spatial gradients of active species and active sites in the catalyst bed of unpromoted and K/Ba-promoted Cu/Al2O3 during CO2 capture-reduction. *J. Mater. Chem. A* **2016**, *4* (18), 6878–6885.
- (84) Al-Mamoori, A.; Lawson, S.; Rownaghi, A. A.; Rezaei, F. Oxidative dehydrogenation of ethane to ethylene in an integrated CO2 capture-utilization process. *Appl. Catal., B* **2020**, *278*, 119329.
- (85) Myint, M.; Yan, B.; Wan, J.; Zhao, S.; Chen, J. G. Reforming and oxidative dehydrogenation of ethane with CO2 as a soft oxidant over bimetallic catalysts. *J. Catal.* **2016**, 343, 168–177.